

# Late Eocene to early Oligocene productivity events in the proto-Southern Ocean and correlation to climate changes drivers of global cooling and Antarctica glaciation

Gabrielle Rodrigues de Faria<sup>1, 2</sup>, David Lazarus<sup>1</sup>, Johan Renaudie<sup>1</sup>, Jessica Stammeier<sup>3</sup>, Volkan Özen<sup>1,2</sup>, Ulrich Struck<sup>1,2</sup>

<sup>1</sup>Museum für Naturkunde, Leibniz Institute for Evolution and Biodiversity Science, Invalidenstraße, 43, Berlin, 10115, Germany

<sup>2</sup>Freie Universität Berlin, Institute for Geological Sciences, Malteserstraße 74-100, Berlin, 12249, Germany

<sup>3</sup>GFZ German Research Centre for Geosciences, Telegrafenberg, Potsdam, 14473, Germany

*Correspondence to:* Gabrielle Rodrigues de Faria (gabrielle.faria@mfn.berlin)

**Abstract.** The Eocene-Oligocene transition (EOT, ca 40-33 Ma) marks a transformation from a largely an-ice-free to an ice-house climate mode that is well recorded by oxygen stable isotopes and sea surface temperature proxies. Opening of the Southern Ocean gateways and decline in atmospheric carbon dioxide levels have been ~~considered~~ hypothesised as factors in this global environmental transformation and the growth of ice sheets in Antarctica possible triggers of the major climate shift during the Cenozoic. A more comprehensive understanding is still needed of the interplay between forcing versus response, the correlation among environmental changes and the involved feedback mechanisms. ~~However, the identification of the driving mechanisms remains controversial and it depends on a better understanding of how the different environmental changes correlate to each other.~~ In this study, we investigate the spatio-temporal variation in export productivity using biogenic Ba (bio-Ba) from ~~different~~ Ocean Drilling Program (ODP) Sites in the Southern Ocean, focusing on possible mechanisms that controlled them as well as the correlation of export productivity changes to changes in the global carbon cycle. We document two significant SO region high export productivity clate-Eocene events in the Southern Ocean during the late-Eocene (ca. 37 and 33.5 Ma) that correlate to proposed gateway-driven changes in regional circulation, and to are correlated to pronounced changes in global atmospheric  $p\text{CO}_2$  levels. Our findings suggest. ~~We propose~~ that paleoceanographic changes that followed Southern Ocean gateway openings, along with more variable increases in circulation driven by episodic Antarctica ice sheet expansion, e and decline of the Antarctic ice sheet, drove enhanced SO export production in the Southern Ocean from the late Eocene through basal Oligocene. These factors may have played a role in emay have driven the episodic reduction of atmospheric carbon dioxide reduction, contributing and contributed to Antarctic glaciation during the Eocene-Oligocene transition.

## 1 Introduction

### 1.1 ~~The~~ Late Eocene Events as Precursor to Antarctic Eocene/Oligocene Boundary Glaciation

The Eocene-Oligocene transition (EOT, ~ 40-33 Ma) is the most important climatic interval of the Cenozoic era (Westerhold et al., 2020 ~~Kennett, 1977; Miller et al., 2009~~). This interval involves profound transformations in environmental conditions including the onset of continental-scale Antarctica glaciation at the Eocene-Oligocene boundary (Shackleton & Kennett, 1975, Zachos et al., 1996, Coxall et al., 2005), sea-level fall (Houben et al., 2012) and global cooling (Prothero and Berggren, 1992; Liu et al., 2009; Bohaty et al., 2012; Hutchinson et al., 2021) as

36 evidenced by a global shift in oxygen isotope records from biogenic calcium carbonate ( $>1\%$ ; Zachos et al. 2001;  
37 Coxall et al. 2005; Bohaty et al., 2012; Westerhold et al., 2020). A positive deep-sea carbon isotope excursion of up to  
38  $1\%$  (Zachos et al., 2001, Coxall et al., 2005; Coxall and Wilson, 2011; Westerhold et al., 2020) and a change from a  
39 shallow ( $\sim 3.5$  km) to a deeper ( $\sim 4.5$  km) calcite compensation depth (CCD) (Coxall et al., 2005; Rea and Lyle, 2005;  
40 Pälke et al., 2012; Dutkiewicz and Müller, 2021; Taylor et al., 2023) have also been observed and indicate that the  
41 carbon cycle played an important role in the changes observed during the transition, although the mechanisms that  
42 caused the carbon cycle perturbation are still unsolved.

43 Carbon cycling acts through a variety of feedback mechanisms. Even though it is well recognized that changes in  
44 atmospheric carbon dioxide ( $\text{CO}_2$ ) impact the Earth's climate because of its large effect on temperature (Arrhenius,  
45 1896; IPCC, 2021), the mechanisms controlling  $\text{CO}_2$  levels over long timescales are still a matter of debate. [A simplified carbon cycle theory suggests that the level of  \$\text{CO}\_2\$  is expected to remain in a steady state over multi](#)  
46 [millennial \( \$>10\$  kyr\) timescales \(Berner et al., 1983; DeVries, 2022\). This stability is attributed to a dynamic interplay](#)  
47 [of transfer of carbon between volcanic inputs, oceans, atmosphere and sequestration in marine sediments involving](#)  
48 [several mechanisms such as weathering, volcanism, and the ocean's biological pump.](#)

49 [However, the Earth's  \$p\text{CO}\_2\$  has, in fact, undergone substantial changes, from Glacial-Interglacial timescales \(Sigman &](#)  
50 [Boyle, 2000\) to long term changes during the Cenozoic \(Beerling and Royer, 2011; Anagnostou et al., 2016\), thus](#)  
51 [suggesting that the Earth's carbon system operates in a more complex way than proposed in the canonical model.](#)

52 [Changes in the Southern Ocean productivity are thought to have altered  \$p\text{CO}\_2\$  levels in the Earth's past, specifically on](#)  
53 [Glacial-Interglacial timescales \(Archer et al., 2000; Sigman et al., 2010\), although magnitude and timing remain](#)  
54 [debated. Changes in the late-Eocene Southern Ocean export productivity over 1 million years, as documented in our](#)  
55 [research, could potentially have impacted  \$\text{CO}\_2\$  levels, as hypothesized by Egan et al., \(2013\), based on Si isotope proxy](#)  
56 [data for Paleogene Southern Ocean diatom productivity.](#)

57 The carbon cycle perturbation at the EOT provides an opportunity to understand climate-carbon cycle feedback (Zachos  
58 and Kump, 2005). The mechanisms proposed to explain such perturbations are processes operating gradually over long  
59 timescales, and may have had their origins in the middle to late Eocene. Preceding the abrupt change at the E/O  
60 boundary, the late Eocene was a period of gradual cooling and progressive  $\text{CO}_2$  levels decrease (Lauretano et al., 2021).  
61 The events associated with this time period may have had substantial importance in pre-conditioning the climate system  
62 prior to the major climatic shift at the E/O boundary (Egan et al., 2013). The potential main drivers for the initiation of  
63 this global cooling and ice build-up in Antarctica are actively debated. [Declining global atmospheric carbon dioxide](#)  
64 [concentrations, and the opening of Southern Hemisphere oceanic gateways, namely the Drake Passage \(DP\) and the](#)  
65 [Tasmanian Gateway \(TG\), are often proposed hypotheses to explain this transition \(Coxall and Pearson, 2007; DeConto](#)  
66 [et al. 2008\). The decline of carbon dioxide levels is an important factor in driving cooler temperatures, and has been](#)  
67 [suggested as the crucial factor in the EOT cooling and subsequent build-up of continental glaciers on Antarctica](#)  
68 [\(DeConto and Pollard, 2003; Huber and Nof, 2006; Pagani et al., 2011\). Atmospheric  \$\text{CO}\_2\$  partial pressure \( \$p\text{CO}\_2\$ \)](#)  
69 [decline has robust observational support. Atmospheric  \$p\text{CO}\_2\$  has been shown to decline through the Eocene, from ca](#)  
70 [1400 p.p.m. at the Early Eocene Climate Optimum \(EECO, ca 51 to 53 million years ago\) to about 770 p.p.m. in the](#)  
71 [late-Eocene reaching a minimum of  \$550 \pm 190\$  p.p.m. in the early Oligocene \(Anagnostou et al. 2016\). However, data is](#)  
72 [noisy, with significant variations among different proxies and thus details of the magnitude and timing are still unclear.](#)  
73 [Furthermore, the  \$\text{CO}\_2\$  threshold \( \$\sim 780\$  p.p.m.v\) needed for the onset of Antarctica glaciation, is highly dependent on](#)  
74

75 model boundary conditions while ice sheet model simulations reveal inter-model disagreement (Gasson et al., 2014).  
76 Therefore, it is crucial to approach this leading hypothesis with caution due to these uncertainties.  
77 The tectonic opening of the Southern Ocean gateways is considered a mechanism contributing to the climatic shift  
78 because it allows the initiation of a circum-Antarctic flow, leading to the formation of the Antarctic Circumpolar  
79 Current (ACC) (Kennett, 1977; Barker, 2001; Scher and Martin, 2006; Toumoulin et al. 2020). This intense eastward  
80 flowing current is proposed in this hypothesis to impact the regional and global climate by preventing tropical heat of  
81 low latitudes from reaching Antarctica, promoting the thermal isolation of Antarctica. Numerous ocean circulation  
82 model studies of this hypothesis have yielded conflicting results (Mikolajewicz et al., 1993; Najjar et al., 2002; De  
83 Conto & Pollard, 2003; Sijp et al., 2009; Goldner et al., 2014; Ladant et al., 2014; Inglis et al., 2015) but most of these  
84 earlier works were limited by unrealistic boundary conditions or other issues (Toumoulin et al., 2020, Hutchinson et al.,  
85 2021). Recent modelling circulation studies (e.g. Toumoulin et al., 2020; Sauermilch, et al. 2021) demonstrate the  
86 importance of the Southern gateway openings and the proto-ACC on ocean cooling in the Southern Hemisphere.  
87 Additionally, glaciation has itself a strong influence both on the circulation of the Southern Ocean and on global  
88 climate, via increased albedo, colder temperatures and increased latitudinal temperature gradients, and stronger zonal  
89 winds (Goldner et al., 2014). There is increasing evidence for at least partial, if transient Antarctic continental glaciation  
90 within the late Eocene (Scher and Martin, 2014), and thus this also needs to be considered in understanding how climate  
91 and ocean change developed within this period.

92 The potential main drivers for the initiation of this global cooling and ice build-up in Antarctica are actively debated.  
93 Declining global atmospheric carbon dioxide concentrations, and the opening of Southern Hemisphere oceanic  
94 gateways, namely the Drake Passage (DP) and the Tasmanian Gateway (TG), are the two main proposed hypotheses to  
95 explain this transition (Coxall and Pearson, 2007; DeConto et al. 2008). The decline of carbon dioxide levels are an  
96 important factor in driving cooler temperatures, and have been suggested as the crucial factor in the EOT cooling and  
97 subsequent build-up of continental glaciers on Antarctica (DeConto and Pollard, 2003; Huber and Nof, 2006; Pagani et  
98 al., 2011). Atmospheric CO<sub>2</sub> partial pressure ( $p\text{CO}_2$ ) decline has observational support during the E/O boundary by  
99 independent proxies, showing levels falling below 800 ppm (Pearson, 2009; Pagani et al. 2011; Zhang et al., 2013;  
100 Anagnostou et al. 2016), although data is sparse and thus details of the magnitude and timing are still unclear.  
101 Atmospheric  $p\text{CO}_2$  has shown to decline through the Eocene, from ca 2000 ppm in the Middle Eocene (Bijl et al., 2010)  
102 to ca. 1000 ppm in the latest Eocene (Pearson et al., 2009). While  $p\text{CO}_2$  reconstructions have advanced, there is marked  
103 variation between different proxies and the absence of tighter constraints on causative mechanisms requires further  
104 investigation of the carbon-climate interactions.

105 The tectonic opening of the Southern Ocean gateways is considered a trigger mechanism of the climatic shift because it  
106 allows the initiation of the Antarctic Circumpolar Current (ACC) (Kennett, 1977; Barker, 2001; Scher and Martin,  
107 2006; Toumoulin et al. 2020). This intense eastward flowing current is proposed in this hypothesis to impact the  
108 regional and global climate by preventing tropical heat of low latitudes from reaching Antarctica, promoting the thermal  
109 isolation of Antarctica (Kennett and Shackleton, 1976). Numerous ocean circulation model studies of this hypothesis  
110 have yielded conflicting results (De Conto & Pollard, 2003; Goldner et al., 2014; Inglis et al., 2015; Ladant et al., 2014;  
111 Mikolajewicz et al., 1993; Najjar et al., 2002; Sijp et al., 2009) but most of these earlier works were limited by  
112 unrealistic boundary conditions or other issues (Toumoulin et al., 2020, Hutchinson et al., 2021). Recent modelling  
113 circulation studies (e.g. Toumoulin et al., 2020; Sauermilch, et al. 2021) demonstrate the importance of the Southern  
114 gateway openings and the proto-ACC on ocean cooling in the Southern Hemisphere. Additionally, glaciation has itself a

115 ~~strong influence both on the circulation of the Southern Ocean and on global climate, via increased albedo, colder~~  
116 ~~temperatures and increased latitudinal temperature gradients, and stronger zonal winds (Goldner et al., 2014). There is~~  
117 ~~increasing evidence for at least partial, if transient Antarctic continental glaciation within the late Eocene (Seher and~~  
118 ~~Martin, 2014), and thus this also needs to be considered in understanding how climate and ocean change developed~~  
119 ~~within this period.~~

120 In addition to the above physical impacts Moreover, the ACC is associated with the development of the Southern Ocean  
121 fronts that contribute to upwelling-induced biological productivity (Chapman et al., 2020). Considering that the changes  
122 in the Southern Ocean circulation have the potential to affect export productivity and via its link to carbon sequestration  
123 in sediments, the role of export productivity in removing  $p\text{CO}_2$  from the ocean-atmosphere system, the 'CO<sub>2</sub>' hypothesis  
124 and the 'tectonic' hypothesis may be linked, via the influence that gateways may have had on Southern Ocean  
125 circulation, increasing export productivity enough to affect global  $p\text{CO}_2$  (Egan et al., 2013). Therefore, evaluating  
126 export productivity patterns in the Southern Ocean across the Eocene-Oligocene and its relationship with circulation  
127 and decline of atmospheric carbon dioxide during this time period provide important information about possible  
128 climate feedbacks in this prominent climatic transition.

129 Many studies have shown variations in biological productivity during at this time interval (Diester-Haass, 1995; Diester-  
130 Haass and Zahn, 1996; 2001, Salamy and Zachos, 1999; Diester-Haass and Zachos, 2003; Schumacher and Lazarus,  
131 2004; Anderson and Delaney, 2005; Villa et al., 2014), pointing towards a productivity increase associated with ocean  
132 circulation changes that increased surface water nutrient availability (Diester-Haass 1992; Zachos et al 1996). However,  
133 existing studies have mostly focused on a single sites, whose paleoceanographic history may reflect local rather than  
134 regional developments. A much broader spatial investigation is particularly important for understanding the influence of  
135 large-scale ocean circulation on this process. Moreover, the timing of productivity changes differs among the studies  
136 and different proxies, limiting our understanding of cause-and-effect relationship. This h, therefore, highlights  
137 the importance of well constrained age models and use of consistent paleoproductivity proxies.

138 Here, we reconstruct changes in export productivity in the Southern Ocean across the late Eocene and early Oligocene,  
139 and evaluate how the changes observed may be linked to ocean circulation changes and how they may have contributed  
140 to the climate changes observed at this interval. We utilize biogenic barium (bio-Ba) accumulation rates to measure  
141 marine export productivity. Bio-Ba is defined as the fraction of total barium that is not associated with terrigenous  
142 sources, sometimes referred to as excess-Ba (Dymond et al., 1992), and has been applied in several studies in the  
143 Paleogene (eg. Nielsen et al., 2003; Anderson and Delaney, 2005; Faul and Delaney, 2010). It is considered a relatively  
144 reliable proxy to estimate changes in paleoproductivity in the Southern Ocean. Newly generated carbon and oxygen  
145 stable isotope records from the same samples of our bio-Ba data further constrain possible causative mechanisms for the  
146 climatic shift at the EOT. We compare our export productivity proxy results to indicators of ocean circulation change,  
147 such as Neodymium (Nd) isotopes. Neodymium isotopes have emerged as a valuable geochemical water mass tracer  
148 (Piepgras and Wasserburg, 1982; Martin and Haley, 2000, Roberts et al., 2010), contributing significantly to our  
149 understanding of the role of ocean circulation in the geological past. This proxy provides an opportunity to asses the  
150 origin of water masses and reconstruct deep ocean circulation. Here, we use Nd isotope data to help understand gateway  
151 opening, paleoceanographic changes and ice sheet history during the Eocene-Oligocene transition, and how these  
152 changes may have influenced marine biological productivity. We also compare our productivity records to well  
153 established proxies for the global carbon cycle, specifically  $p\text{CO}_2$  and  $\delta^{13}\text{C}$  of benthic deep sea foraminifera.

154 Here, we reconstruct the changes in export productivity across the late Eocene and early Oligocene, and evaluate how  
155 the changes observed may be linked to ocean circulation changes and contributed to the climate changes observed at  
156 this interval.

157 Newly generated carbon and oxygen stable isotope records from the same samples of our *bio*-Ba data constrain the  
158 question of the causative mechanisms for the climatic shift at the EOT. We compare our export productivity proxy  
159 results to indicators of ocean circulation change, including how these changes correspond with gateways opening,  
160 paleoceanographic changes, ice sheet history, and their influence on marine biological productivity. We also compare  
161 our productivity records to proxies for the global carbon cycle, specifically  $p\text{CO}_2$  and  $\delta^{13}\text{C}$  of benthic deep sea  
162 foraminifera. Advancing our understanding of the cause of this event is crucial in identifying the mechanisms governing  
163 global climate change.

164 Our ~~u~~Although much of our understanding of the Eocene-Oligocene transition has been ~~enhanced~~achieved through  
165 modelling studies as they provide means to compare several possible scenarios ~~and generate ‘data’ for components of~~  
166 ~~the system for which no direct proxy data is available. However, all models are simplifications of complex, not fully~~  
167 ~~understood systems; and are dependent on parameterizations~~parametrizations and calibrations to often sparse, noisy  
168 ~~proxies that ground-truth model outputs. T~~, this paper ~~instead~~ focuses on proxy evidence of the changes that occurred in  
169 this time interval. Our ~~multi~~proxy approach and wide coverage allow us to test the hypotheses:

170 H1: Changes in ocean circulation patterns that took place during the late Eocene and early Oligocene (eg. development  
171 of ACC and strengthening of AMOC) contributed to the increase in biological productivity in the Southern Ocean.

172 H2: The magnitude of the export productivity increase during a time period that preceded the EOT may have been an  
173 important contribution to the drawdown of  $p\text{CO}_2$ .

174 First, we investigate the export productivity changes across the late Eocene to early Oligocene in two different regions  
175 in the Southern Ocean. Then we compare our results to the paleo-circulation changes that occurred at the same time  
176 period. We conclude by summarising the implications of the changes in ocean circulation and the possible climate  
177 driving mechanisms that led to the cooling of Earth.

## 178 | 1.2. Paleooceanographic Setting

179 The Southern Ocean (SO) today is an important part of the global ocean circulation and climate system, interconnecting  
180 the Atlantic, Pacific and Indian Ocean basins, providing and thus inter-basin exchange of ocean properties and heat  
181 ([Rintoul et al., 2001](#)). There are strong latitudinal gradients and seasonal changes in ocean properties which affect  
182 surface water and export productivity, and thus this region’s role in global carbon capture and sequestration. Low light  
183 levels and, in higher latitudes, extensive sea ice limit productivity during the winter months. Deep surface mixed layers  
184 over the large areas of the Southern Ocean, beyond the shallow stratification effects of meltwater near the sea ice edge,  
185 also tend to limit productivity in spring through fall as plankton is mixed below critical thresholds of light availability  
186 ([Deppeler and Davidson, 2017](#)). The relationship between mixed layer thickness and productivity however is complex  
187 (Nelson and Smith, 1991; Li et al. 2021). Southern Ocean productivity is thus concentrated near the Antarctic  
188 Circumpolar Current (ACC), the dominant current in the region. This current is the longest and strongest ocean current  
189 on Earth. This complex circulation system is driven mainly by westerly winds, resulting in Ekman transport and  
190 favouring deep water upwelling. This flow pattern is possible in the absence of land barriers and is ~~governed~~balanced



191 | by ~~bathymetry bottom topography friction~~ (Rintoul et al., 2001; Carter et al., 2008), while the strength of the current is  
192 | driven by the strength and location of the westerly winds, and thus, among other factors, the global latitudinal thermal  
193 | gradient. The ACC is a key component of the ‘ocean conveyor belt’, playing a role in the global transport of heat  
194 | (~~Rintoul et al., 2001~~; Katz, et al. 2011). Moreover, this circumpolar current influences the strength of meridional  
195 | overturning circulation and several authors have proposed that this current is one of the main drivers of the Atlantic  
196 | meridional overturning circulation (AMOC) (Toggweiler and Samuels, 1995; Toggweiler and Bjornsson, 2000; Scher  
197 | and Martin, 2006, Kuhlbrodt et al., 2007, Scher et al., 2015, Sarkar et al., 2019).

198 | The ACC is structured of multiple hydrological fronts, associated with specific water mass properties such as  
199 | temperature and salinity (Sokolov and Rintoul, 2009). Orsi et al., 1995 ~~were the first to proposed~~ the traditional view of  
200 | Southern Ocean fronts. It consists of the Subantarctic Front (SAF), the Antarctic Polar Front (APF) and the Southern  
201 | ACC Front (SACCF). Besides these main fronts, a Subtropical Frontal Zone (STFZ) can be found north of the ACC  
202 | (Orsi et al., 1995; Palter et al. 2013; Chapman ~~et al.~~, 2020). This frontal structure is fundamental to different processes  
203 | that occur in the region, such as the distribution of important nutrients through the exchange between deep and surface  
204 | ocean, and the exchange of tracers (Palter et al., 2013). Upwelling of Circumpolar Deep Water (CDW) brings nutrient-  
205 | rich waters to the surface towards the Polar Front Zone (PFZ) where Antarctic Surface Waters (AASW) sink to form  
206 | Antarctic Intermediate Water (AAIW), thereafter it extends into the Subantarctic Zone (SAZ) (Sarmiento et al., 2004)  
207 | (Figure 1).

208 | Wind-driven upwelling, that occurs within the Southern Ocean fronts, enhances biological productivity in these regions  
209 | (De Baar et al., 1995; Moore et al., 1999). More recently, upwelling related to ACC bathymetry has been found as an  
210 | important mechanism for establishing phytoplankton blooms in the SO (Sokolov and Rintoul, 2007). This complex  
211 | structure involving ACC fronts, westerlies and the bottom topography, makes the Southern Ocean a highly productive  
212 | region. Iron remobilisation has also been shown to occur due to latitudinal variations of the ACC (Kim et al., 2009),  
213 | ~~hencee~~ inducing ~~ia massive~~ increases in productivity.

214 | ~~The conventional assumption is that the ACC structure began to develop during the Cenozoic, with the opening of the~~  
215 | ~~Southern Ocean pathways between South America and Antarctica and the following formation of the Drake Passage~~  
216 | ~~(DP) and, also between Australia and Antarctica that allows the Tasmanian Gateway (TG) opening. Removing these~~  
217 | ~~geographic barriers permitted a gradual development of circumpolar flow (Toggweiler and Bjornsoon, 2000). The TG~~  
218 | ~~opening to intermediate and deep waters occurred in the late Eocene, ca 35.5 Ma (Stickley et al., 2004). In contrast,~~  
219 | ~~tectonic reconstructions for the timing of the Drake Passage opening remain controversial, ranging from the late Eocene~~  
220 | ~~(ca 41 Ma; Scher and Martin, 2004, 2006) to the late Oligocene (ca 26 Ma, Barker and Thomas 2004, Hill et al., 2013)~~  
221 | ~~for shallow water exchange. Some studies pointed to deep water exchange occurring as late as the earliest Miocene (ca~~  
222 | ~~22-23 Ma, Barker 2001; Lyle et al., 2007). Even if the timing of the deepening of the Drake Passage is less well~~  
223 | ~~constrained, a “proto-ACC” has been proposed as an earlier expression of the ACC and it is defined as a shallow-depth~~  
224 | ~~circumpolar current (Scher et al., 2015, Sarkar, et al., 2019). Cramer et al. 2009 suggested that “proto-ACC” would~~  
225 | ~~have played an important role in the ocean circulation changes that occurred in the Eocene. Furthermore, even a~~  
226 | ~~relatively shallow proto-ACC would have strongly affected surface water phyto- and zooplankton (Lazarus and Caulet,~~  
227 | ~~1994), and thus potentially the mechanisms of surface water productivity in the region.~~

228 | ~~During the Cenozoic, the ACC structure began to develop with the opening of the pathways between South America and~~  
229 | ~~Antaretica and the following formation of the Drake Passage (DP) and, also between Australia and Antaretica that~~  
230 | ~~allows the Tasmanian Gateway (TG) opening. Removing these geographic barriers permitted the gradual development~~

231 of circumpolar flow (Toggweiler and Bjornsson, 2000). The TG opening to intermediate and deep waters occurred in  
232 the late Eocene, ca 35.5 Ma (Stieckley et al., 2004). Tectonic reconstructions for the Drake Passage timing opening  
233 remain controversial, ranging from the late Eocene (ca 41 Ma; Scher and Martin, 2004, 2006) to the early Miocene (ca  
234 23 Ma, Barker 2001). Even if the timing of the deepening of the Drake Passage is less well constrained, a “proto-ACC”  
235 has been proposed as an earlier expression of the ACC and it is defined as a shallow-depth circumpolar current (Scher  
236 et al., 2015, Sarkar, et al., 2019). Cramer et al. 2009 suggested that “proto-ACC” would have played an important role  
237 in the ocean circulation changes that occurred in the Eocene.

238 Many climate model studies have contributed ~~with~~ insights into the ocean structure and circulation of the late Eocene  
239 (e.g. Huber et al. 2004, Huber & Not 2006, Sijp et al., 2011, Sijp et al., 2016, Elsworth et al., 2017, Baa ~~ts~~sten et al.,  
240 2020; Toumoulin, et al., 2020; Sauermilch et al., 2021; Nooteboom et al., 2022). Although some of these experiments  
241 have shown that opening of gateways was not sufficient to have caused the global cooling recorded by proxies  
242 (DeConto & Pollard, 2003, Huber et al. 2004, Huber & Not 2006, Sijp et al., 2011, Baa ~~ts~~sten et al., 2020), they  
243 acknowledge that the circulation patterns have changed during the Eocene. A recent model circulation experiment has  
244 demonstrated a significant regionalthe impact of the DP opening and its effects on ocean structure and dynamics even  
245 for shallow depths (Toumoulin et al., 2020).

246 The organisation of Southern Ocean proto-oceanic fronts may have occurred during the late-Eocene as shown by  
247 microfossil biogeographic data (Lazarus and Caulet, 1994; Cooke et al., 2002). This and formed poleward (proto-PF:  
248 ←70–60°S; proto-STF: 65–50°S) of their present-day positions, progressing to lower latitudes during the Oligocene  
249 and Miocene (Lazarus and Caulet, 1994; Nelson and Cooke, 2001; Cooke et al., 2002). This frontal system  
250 organizationzone migration likely played a role in major changes at that time period, including higher ocean  
251 productivity.

252 Evidence of significant events during the late Eocene highlights the importance of this period that preceded the  
253 permanent glaciation in Antarctica. An interval of increasingly heavy global benthic oxygen isotope values in the late  
254 Eocene, at ca 37 Ma have been interpreted to reflect pre-EOT glaciation and cooling, this episode is referenced as  
255 PrOM event (Priabonian Oxygen isotope Maximum, Scher et al., 2014). Additional evidence for a prominent cooling  
256 episode has been found during this time period (Anderson et al., 2011; Douglas et al., 2014). Despite uncertainties  
257 about the nature and extent of the earliest ice in Antarctica, these changes imply that paleogeographic reconfiguration  
258 has affected the late Eocene Antarctic climate and it is likely that a com. ~~It is clear that some combination of~~  
259 processes favoured the development of permanent glaciation in Antarctica.

260 Given the importance of changes during the Eocene-Oligocene time interval, especially the ACC development and its  
261 frontal structure to the climate system and ecosystems, it is crucial to investigate the timing and magnitude of late  
262 Eocene paleoceanographic changes in the Southern Ocean, and equally important to expand our understanding of the  
263 implications of such changes on paleoproductivity and how these mechanisms are linked to a changing climate.

264 Our multiproxy approach and wide coverage allow us to test the hypotheses:

265 H1: Changes in ocean circulation patterns that took place during the late Eocene and early Oligocene (eg. development  
266 of a proto-ACC and strengthening of AMOC) contributed to the increase in biological productivity in the Southern  
267 Ocean.

268 H2: The export productivity increase that preceded the EOT may have been temporally correlated to, and thus may have  
269 contributed to the drawdown of  $p\text{CO}_2$ .

270 First, we investigate the export productivity changes across the late Eocene to early Oligocene in three different regions  
 271 in the Southern Ocean. Then we compare our results to the paleo-circulation changes that occurred at the same time  
 272 period, and lastly compare our productivity records to the temporal pattern of change in Eocene-Oligocene  $p\text{CO}_2$ . We  
 273 conclude by summarising the implications of the changes in ocean circulation and the possible climate driving  
 274 mechanisms that led to the cooling of Earth.

## 275 | 2 Materials and Methods

### 276 | 2.1 Site Descriptions

277 We investigated sediment samples from 3 Ocean Drilling Program (ODP) Sites in the Southern Ocean (Table 1). ODP  
 278 ~~Leg-177~~ Site 1090 on the southern flank of the Agulhas Ridge in the Southern Atlantic Ocean (42°54.8'S, 8°53.9'E,  
 279 water depth 3,702m), ODP ~~Leg-133~~ Site 689 on the southern flank of the Maud Rise in the Southern Atlantic Ocean  
 280 (64°31'S, 3°6'E, water depth 2,253m) and ODP ~~Leg-120~~ Site 748 on the southern part of the Kerguelen Plateau in the  
 281 Southern Indian Ocean (58°26.45'S, 78°58.89'E, water depth 1,290.9m). All the sites lie on topographic highs. The  
 282 Agulhas Ridge comprises an elongate part of the Agulhas-Falkland Fracture Zone (AFFZ). The ridge rises ~ 3000m  
 283 above the surrounding floor and constitutes a topographic barrier, having a strong influence on the exchange of water  
 284 masses (Gruetzner & Uenzelmann-Neben, 2015) between high and lower latitudes. The Maud Rise is a seamount, its  
 285 elevation rises almost 3000 m from the seafloor (Brandt et al., 2011). Kerguelen Plateau is a large topographic high in  
 286 the Indian sector of the Southern Ocean. We selected samples from the middle Eocene through the E-O boundary,  
 287 depending on the sample availability.

288 Currently, the sites studied are located in the Southern Ocean through the ACC. Site s 689 is located well south of the  
 289 Polar Front Zone (PFZ), and and 748 slightly to are located in the south of the ~~Polar Front zone (PFZ)~~ and Site 1090 in  
 290 the Subantarctic zone, between the Subtropical front (STF) and the Subantarctic Front (SAF) (Figure 1). Across the  
 291 Eocene-Oligocene transition, the sites were shallower (Table 1), ranging between ca 1.2 and 3 km paleo water depth.  
 292 These depths are well suited to capture signals of export productivity to intermediate-deep waters. Sites 689 and 748  
 293 locations were similar to today and site 1090 was as much as 5° farther to the south (Gersonde et al., 1999) (Table 1).

294 The major lithology from the lower Eocene to the upper Oligocene at the Maud Rise is composed of calcareous and  
 295 silicious oozes (Barker et al., 1988). Kerguelen Plateau site is composed mainly of nannofossil ooze and chert (Barron  
 296 et al., 1989). Agulhas Ridge is predominantly composed of diatoms and nannofossil ooze, with  $\text{CaCO}_3$  wt% highly  
 297 variable, ranging from non-detectable to 69% of sediment throughout the study interval. (Gersonde et al., 1999) with  
 298 rare occurrences and barren intervals of planktic and benthic foraminifera making it difficult to establish stable isotope  
 299 records ~~at~~ this site.

300 **Table 1.** Position of the ODP Sites studied in the present-day and in the late-Eocene (~ 37 Ma). Paleocoordinates  
 301 calculated based on Seton et al. (2012) rotation model.

Site	Geographic Setting	Latitude	Longitude	Water depth (m)	Paleodepths (m)	Paleo-latitude	Paleo-longitude
1090	Agulhas Ridge	42°54.8'S	8°53.9'E	3 702	ca. 3,000-3,300 (Pusz et al. 2011)	ca 47°33'S	ca 1°46.8' E
689	Maud Rise	64°31'S	3°6'E	2 253	ca. 1500	ca 64°19.2'S	ca 2°43.2' E



					(Diester-Haass and Zahn, 1996)		
748	Kerguelen Plateau	58°26.45'S	78°58.89'E	1 290.9	ca. 1200 (Wright et al., 2018)	ca 56°48.6'S	ca 75°36' E

## 302 2.2 Age Models, Linear Sedimentation Rates

303 Revised age models for the ODP Site 1090, ODP Site 689 and ODP Site 748 ~~made for~~ this study were based on all  
304 magnetostratigraphic and biostratigraphic data available, ~~and both models and data are available from~~ the Neptune  
305 database ~~via~~ NSB system (Renaudie et al., 2020) (Figures S1-S4). All ages in our study are given in the GPTS standard  
306 used by NSB (Gradstein et al. (2012) ~~GPTS scale~~, or have been remapped to this scale from prior studies. Differences  
307 between this and more recent GPTS scales in the Cenozoic are minor, and generally less than other age model  
308 uncertainties for the sections in our study.

309 ODP Site ~~177~~ 1090 has an age model constructed from shipboard magnetostratigraphic ~~data~~ “U-channel”  
310 measurements, and the records fit well to the geomagnetic polarity timescale (GPTS) (Channell et al., 2003).  
311 Nannofossil biostratigraphy has confirmed the Chron ages (Marino and Flores, 2002), as well as foraminiferal  
312 biostratigraphy (Galeotti et al. 2002), strontium isotopes (Channell et al., 2003) and oxygen and carbon isotope data  
313 from benthic foraminifera (Zachos et al., 2001; Billups et al., 2002). This integration of several age indicators and their  
314 consistency makes this a robust and very well constrained age model.

315 Magnetostratigraphic data for ODP ~~H3~~ Site 689 is partially reinterpreted from the measurements originally made by  
316 Spiess, 1990. A new high-resolution study of Eocene-Oligocene “U-channel” samples from this site shows ~~apresents~~  
317 high correlation with the GPTS (Florindo and Roberts, 2005). Ca ~~Ocean~~ calcareous nannofossil datums (Wei and Wise,  
318 1992; Wei, 1992, Persico and Villa, 2002, 2004), planktonic foraminiferal datums (Kennett and Sott, 1990; Thomas,  
319 1990; Berggren et al., 1995) and Argon-argon (<sup>40</sup>Ar/<sup>39</sup>Ar) dating (Glass et al., 1986; Vonhof et al., 2000) are ~~is~~ used to re-  
320 calibrate ages for this site.

321 A high-resolution magnetostratigraphic study from ODP Site 748B was carried out by Roberts et al. 2003 in continuous  
322 “U-channel” samples, revising the shipboard analysis from Inokuchi and Heider, 1992. Calcareous nannofossils  
323 biostratigraphy (Aubry 1992), planktonic foraminiferal biostratigraphic datums (Berggren et al., 1995), diatom datums  
324 (Baldauf and Barron, 1991, Roberts et al., 2003) and strontium isotopes ages (Zachos et al., 1999; Roberts et al., 2003)  
325 were re-evaluated for a better age model.

326 Accumulation rate fluxes are obtained by calculating the product of linear sedimentation rates (LSR) and shipboard  
327 measured dry bulk densities (DBD), thus a robust age model is crucial for this calculation because it determines the  
328 linear sedimentation rates. We use ~~present data using~~ a straightforward LSR calculation between age-depth control  
329 points based on magnetostratigraphic data, stable isotopes and biostratigraphic data. Mass accumulation rates (MARs,  
330 mol cm<sup>-2</sup> kyr<sup>-1</sup>) were calculated using LSR based on the above age models multiplied by DBD.

331 Since bio-Ba AR is a direct function of LSR, it is essential to evaluate any possible biases due to this ~~influence~~. Figure  
332 S5 shows a comparison of linear sedimentation rates and bio-Ba AR. This comparison showed a high amplitude peak at  
333 ODP Site 1090, with LSR of 4.11 cm kyr<sup>-1</sup> at the late Eocene, this high rate is based on a very constrained model. The  
334 LSRs for ODP Site 689 vary ~~ies~~ from 0.1 cm kyr<sup>-1</sup> during the early Oligocene to up to 1.3 cm kyr<sup>-1</sup> in the late Eocene,

335 | whereas ODP Site 748 has more uniform values during the late Eocene. Small adjustments to LSRs may result in large  
336 | changes in MARS, emphasising the importance of very well constrained age models. The available age data for our sites  
337 | allow some variation in the placement of the line of correlation, and thus the precise timing and magnitude of  
338 | sedimentation rate changes on the scale of  $\pm$  ca 0.5 m.y. are not well constrained. P-p patterns and calculated values over  
339 | longer time scales are however thought to be robust.

### 340 | 2.3 Stable Isotope Analyses

341 | Stable isotopes of carbon and oxygen were measured both on the bulk fine fraction ( $<45\mu\text{m}$ ) and benthic foraminifera.  
342 | Bulk sediments were oven-dried and washed through different sieve sizes (125 and  $45\mu\text{m}$ ). Smear slides observations  
343 | indicate that the main carbonate composition of the fine fraction is coccoliths, therefore stable isotopic compositions of  
344 | bulk fine fraction ( $<45\mu\text{m}$ ) reflect primarily nannofossil isotope signals. Contamination by non-coccolith carbonate  
345 | such as fragments of foraminifera shells is minimal (Figure S5). Fifteen to twenty tests of benthic foraminifera  
346 | (*Cibicoides* spp.) were picked from the  $>125\text{-}\mu\text{m}$ -size fraction. Foraminiferal tests were ultrasonically cleaned using  
347 | ethanol and oven-dried. Stable isotopic analyses were carried out at the Stable Isotope Laboratory of the Museum für  
348 | Naturkunde (Berlin, Germany) on a Thermo Isotope Ratio Mass Spectrometer. All values are reported in the  $\delta$ -notation  
349 | in parts per mil (‰) relative to the Vienna Pee Dee Belemnite (VPDB). In this study, we applied an adjustment of  
350 |  $+0.64\text{‰}$  (Shackleton and Opdyke, 1973; Shackleton et al., 1984) to all  $\delta^{18}\text{O}$  values of the benthic foraminifera  
351 | *Cibicoides* to account for disequilibrium effects.

### 352 | 2.4 Barium Analyses and Biogenic Barium as a Paleoproductivity Proxy

353 | Barium (Ba) and aluminum (Al) were analysed by ICP OES, performed at the EIMiE Lab at the German Centre for  
354 | Geosciences (GFZ, Potsdam, Germany) using a 5110 spectrometer (Agilent, USA). The analytical precision and  
355 | repeatability were generally better than 2% and it is regularly tested by certified reference material and in-house  
356 | standards. For preparation, 2g of each sample were grounded to assure grain size distribution, and digested by  $\text{Na}_2\text{O}_2$   
357 | fusion and HCl using ultrapure reagents, following the method by Bokhari and Meisel (2017) dissolved with ultra-pure  
358 | HCl. Intensity calibration was performed by external calibration using the same batch of solvent to ensure matrix  
359 | matching. The analytical blank was negligible compared to the sample concentration.

360 | Using barium as a paleoproductivity proxy requires some adjustments because other biogenic sources may contribute to  
361 | the barium content in the sediment. Detrital aluminosilicate may affect the barium signal in Southern Ocean sediments.  
362 | In order to solve this issue and reveal aluminosilicate contributions, the Biogenic Barium calculation was used as  
363 | proposed by Dymond et al., 1992, following Eq (1):

$$364 \quad \text{Biogenic Barium (Bio Ba)} = (\text{Ba total})_{\text{sample}} - (\text{Ba/Al})_{\text{bulk continental crust}} \times \text{Al}_{\text{sample}} \quad (1)$$

365 | This assumes that the aluminum (Al) concentration and the average continental crust abundance are representative of  
366 | the detrital Ba component. The Ba/Al crust ratio of 0.0075 is the global average value from sedimentary rocks as  
367 | suggested by Dymond et al. (1992). This value is based on various compilations of elemental abundances in crustal  
368 | rocks. This normative calculation potentially introduces uncertainty in samples with high and variable detrital barium,

369 but considering that clay assemblages and weathering regimes were relatively constant during the early Paleogene in the  
370 Southern Ocean, therefore, the crustal ratio probably did not vary much (Robert et al. 2002).

## 371 2.5 Data Compilation

### 372 2.5.1 Neodymium Isotope Data

373 Neodymium isotopes in seawater reflect the different weathering sources of neodymium that affects each water mass.  
374 The isotope values act as conservative elements during ocean mixing. They are therefore a robust water mass tracer,  
375 and further are faithfully archived in sediments (Piepgras and Wasserburg, 1982; Martin and Haley, 2000). Their  
376 behaviour in seawater and the conservation of the signal in sediments make them a valuable proxy for  
377 paleoceanographic studies and past ocean circulation reconstruction. Fossilised fish teeth are commonly used and are  
378 considered robust archives to extract Nd isotopic signatures because they incorporate and preserve their Nd signature  
379 during very early diagenesis (Martin and Scher, 2004), and they can be found in deep-sea sediment samples all over the  
380 world and in many geologic time intervals. The Nd signal is given in  $\epsilon\text{Nd}$ , where  $\epsilon\text{Nd}$  is the ratio  $^{143}\text{Nd}/^{144}\text{Nd}$  of a  
381 sample relative to the same of the bulk Earth, in parts per 10,000.

382 In this study, we compiled published Nd isotope data from fossil fish teeth, from the same Ocean Drilling Program  
383 (ODP) sites that we investigated in the Southern Ocean (ODP Site 1090 Agulhas Ridge, [Scher and Martin, 2006](#); ODP  
384 Site 689 Maud Rise, [Scher and Martin, 2004](#); -and ODP Sites [738, 744 and -748 on the Kerguelen Plateau, Scher and](#)  
385 [Delaney, 2010](#); [Scher et al., 2011](#); [Scher et al., 2014](#); [Wright et al., 2018](#)) and explore the Nd isotope variability to  
386 examine the intrusion of waters from the Pacific to the Atlantic sector of the Southern Ocean. We then used these data  
387 and our records to explore the evolution of the Southern Ocean circulation and significant circulation changes across the  
388 Eocene-Oligocene transition. Sources of Nd isotope data are given in Table S1.

### 389 2.5.2 $p\text{CO}_2$ Data

390 A variety of geological proxies have been applied in numerous studies to reconstruct the partial pressure of atmospheric  
391  $\text{CO}_2$  ( $p\text{CO}_2$ ) during the Cenozoic Era (e.g. [Pagani et al., 2005, 2011](#); [Küschner et al., 2008](#); [Retallack et al., 2009](#);  
392 [Beerling & Royer 2011](#), [Anagnostou et al., 2016, 2020](#)). Given the low published sampling density through the critical  
393 Eocene-Oligocene interval, we compiled published  $p\text{CO}_2$  data from marine and terrestrial proxies that have been  
394 identified as reliable for reconstructing  $p\text{CO}_2$  during this period. The marine geochemical proxies include alkenone-  
395 based estimations, carbon and boron isotope ( $\delta^{11}\text{B}$ ) composition of well-preserved planktonic foraminifera calcite.  
396 Proxies from the terrestrial reservoir include Paleosols and Stomatal frequencies. Our atmospheric  $\text{CO}_2$  compilation  
397 (Table S2) consists to our knowledge all the currently available proxy data on Eocene and Oligocene  $p\text{CO}_2$  records,  
398 including all data compiled in previous syntheses through extensive scientific community efforts in paleo  $\text{CO}_2$  database  
399 (The Cenozoic  $\text{CO}_2$  Proxy Integration Project Consortium, 2023), such compilations are commonly used to estimate  
400 past  $p\text{CO}_2$ , although it is known that there are limitations and variation among them (IPCC, 2021). Zhang et al. (2013)  
401 specifically argued that compositing limited, short time interval data from different proxies, and different localities is  
402 likely to introduce significant short-term bias at individual data series end-points into the resulting fitted curve, and  
403 instead generated a 40 My long history of Cenozoic  $p\text{CO}_2$  using a single proxy from a single section (Site 925 in the  
404 equatorial Atlantic). We consider this study's results to be the best and most complete single source of information on  
405 the Cenozoic trend of atmospheric  $p\text{CO}_2$ . However, precisely because of the substantial amounts of between proxies and

406 | between locality variation, data using a single proxy and from a single site is also potentially not representative of  
407 | global  $p\text{CO}_2$  history. We thus use both the single site results of Zhang et al. (2013) and the full, multi-site and multi-  
408 | proxy compilation (Supplementary material) in evaluating our own study's results.

409 | A variety of geological proxies have been applied to reconstruct the partial pressure of atmospheric  $\text{CO}_2$  ( $p\text{CO}_2$ ) during  
410 | the Cenozoic Era (Pearson & Palmer, 2000; Pagani et al., 2005; Beerling & Royer 2011). Given the low sampling  
411 | density through the critical Eocene-Oligocene interval, we compiled published  $p\text{CO}_2$  data from marine and terrestrial  
412 | proxies that have been identified as reliable for reconstructing  $p\text{CO}_2$  in the Cenozoic. The marine geochemical proxies  
413 | include alkenone-based estimations, carbon and boron isotope ( $\delta^{11}\text{B}$ ) composition of well-preserved planktonic  
414 | foraminifera calcite. Proxies from the terrestrial reservoir include paleosol carbon and stomatal density. Our  
415 | atmospheric  $\text{CO}_2$  compilation (Table S2) consists to our knowledge all the currently available proxy data on most recent  
416 | Eocene and Oligocene  $p\text{CO}_2$  records. Such compilations are commonly used to estimate past  $p\text{CO}_2$ , although it is  
417 | known that there are limitations and variation among them (IPCC, 2021). Zhang et al. (2013) specifically argued that  
418 | compositing limited, short time interval data from different proxies, and different localities may introduce substantial  
419 | bias into the resulting fitted curve, and instead generated a 40 Myr long history of Cenozoic  $p\text{CO}_2$  from a single section  
420 | (Site 925 in the equatorial Atlantic). We consider this study's results to be the best single source of information on the  
421 | history of atmospheric  $p\text{CO}_2$ . However, precisely because of the substantial amounts of between proxies and between  
422 | locality variation, data using a single proxy, from a single site is also potentially not representative of global  $p\text{CO}_2$   
423 | history. We thus use both the single site results of Zhang et al. (2013) and the full, multi-site and multi-proxy  
424 | compilation (Supplementary material) in evaluating our own study's results.

## 425 | 3 Results

### 426 | 3.1 Biogenic Barium

427 | Biogenic Barium accumulation rate (bio-Ba AR) records (Figure 2) show a pronounced rise in the late Eocene when the  
428 | values were up to twice as high as in previous periods for all sites studied. At Kerguelen Plateau ODP Site 748, we also  
429 | observe a previous and smaller increase around the middle Eocene Climatic Optimum (MECO, ca 40 Ma). At Maud  
430 | Rise the increase began at ca 38.3 Ma and persisted for around 1.5 Myr. bio-Ba ARs show a high value in the Agulhas  
431 | Ridge at ca 36.8 Ma ~~which that~~ is induced by a high sedimentation rate (Figure S5a). Although export productivity was  
432 | higher (maximum values to about  $16.8 \mu\text{mol bio-Ba cm}^{-2} \text{ky}^{-1}$ ) at Maud Rise compared to the other sites -the Kerguelen  
433 | Plateau reached maximum values of about  $14.3 \mu\text{mol cm}^{-2} \text{ky}^{-1}$  and the Agulhas Ridge site  $13.74 \mu\text{mol cm}^{-2} \text{ky}^{-1}$ , the  
434 | records show a high degree of temporal correspondence in the late Eocene peak (ca 36.8 Ma). Bio-Ba values were low  
435 | at all sites between ca 36 and 34.5 Ma. Between ca 34.5 Ma and ca 33.3 Ma, which includes the EOT interval, bio-Ba  
436 | AR increased in both sites of the Atlantic Sector, but these increases were not very concurrent between the sites  
437 | investigated. On the Agulhas Ridge, ODP Site 1090, the rise in bio-Ba (from  $7.37$  to  $20.46 \mu\text{mol cm}^{-2} \text{kyr}^{-1}$ ) is observed  
438 | in the very latest Eocene (ca 34.3), just before the Oi-1 event. At Maud Rise, ODP Site 689, the increase is not observed  
439 | until ca 1 Myr after, in the early Oligocene (maximum value  $16.25 \mu\text{mol cm}^{-2} \text{kyr}^{-1}$  at ca 33.3 Ma). On the Kerguelen  
440 | Plateau, ODP Site 748, the increase in export productivity registered by bio-Ba during the Oligocene is notably smaller  
441 | than in the Atlantic sites, with values not higher than the low values observed during the Eocene.

442 | Our bio-Ba results are in general concordant with the temporally more limited data obtained by prior studies of  
443 | Southern Ocean sites (Anderson and Delaney, 2005, Site 1090; Diester-Haass and Faul 2019, Site 689) (Figure 2).  
444 | However, our results for Kerguelen Plateau Site 748 differ from those of Faul and Delaney, 2010 for nearby Site 738,  
445 | where the latter estimate bio-Ba accumulation rates up to twice those obtained in our study of Site 748. The differences  
446 | may be due to the different locations of the two sites, Site 738 is located several degrees further south, and in ca 1 km  
447 | deeper water depth. The bio-Ba proxy is also very sensitive to sedimentation rates, and the differences may be due to

448 the poor age control for Site 738 which in ~~the our~~ studied time interval consists only of a few rather scattered  
449 biostratigraphic events (Figure S4a), ~~resulting which results~~ in substantially different age models between our study,  
450 Faul and Delaney (2010), and other recent studies of this site, e.g. Huber and Quillevere (2005). In these studies the  
451 location and extent of hiatuses, and the uniformity of sedimentation rates varies considerably (SOM Figure S4b). The  
452 age model for Site 748 by contrast (Figure S3) is very well constrained by coherent biostratigraphic events from  
453 multiple groups of microfossils, Sr isotope stratigraphy and paleomagnetic stratigraphy, and we therefore accept the  
454 results from Site 748 as being more reliable.

455 When the data for individual sites is composited together, the behaviour of the Southern Ocean region can be roughly  
456 estimated, even though our geographic coverage (lacking data from the Pacific/New Zealand sector) is incomplete and  
457 thus may not be entirely representative of the Southern Ocean as a whole. A lowess curve fit to the composited bio-Ba  
458 data shows that the key patterns noted in individual records are retained in the composite signal, and thus that Southern  
459 Ocean productivity can be characterised as having had two intervals of high values at around 37 and 34 Ma.

### 460 3.2 Oxygen and Carbon Isotopes

461 Our new oxygen (Figure 3C and E) and carbon (Figure 3D and F) stable isotope data allow us to identify previously  
462 noted trends and distinct events during the period studied. Benthic  $\delta^{18}\text{O}$  values exhibit a consistent increasing trend  
463 during the late Eocene indicating the overall decrease of oceanic bottom water temperatures. A sharp increase occurs at  
464 the Eocene-Oligocene transition (between 33.9 and 33.3 Ma) at both sites examined. This rapid shift has been observed  
465 in several sites in the Southern Ocean (e.g., Muza et al., 1983; Miller et al., 1987; Mackensen and Ehrmann, 1992;  
466 Zachos et al., 1996; Billups et al., 2002; Pusz et al., 2011) and it is well established as a global signal (Zachos et al.,  
467 2001). It is generally interpreted as a combination of deep ocean water cooling and major ice growth on the Antarctic  
468 continent (Zachos et al., 2001). At Site 689, the planktic  $\delta^{18}\text{O}$  curve almost mimics the benthic one. The  $\delta^{18}\text{O}$  values  
469 measured on fine fraction reveal a heavier trend more pronounced at ODP Site 748 (Kerguelen Plateau) compared to  
470 ODP Site 689 (Maud Rise). During the late Eocene, around 37 Ma, heavier  $\delta^{18}\text{O}$  values are observed in both the Atlantic  
471 and Indian Sectors of the SO, the benthic/fine fraction ratio declines, indicating more homogenous temperature in the  
472 water column. Both benthic and planktic foraminifera  $\delta^{13}\text{C}$  records show fluctuations across the period studied, with  
473 low values across the Eocene-Oligocene boundary, followed by an increase that accompanied the  $\delta^{18}\text{O}$  increase and low  
474 values again in the upper Oligocene. The benthic trend is also observed by previous data from the same sites  
475 (Mackensen and Ehrmann, 1992; Diester-Haass and Zahn, 1996; Bohaty et al., 2003). The fine fraction records show  
476 elevated  $\delta^{13}\text{C}$  values between Late Eocene to Early Oligocene, followed by a decreasing trend during the Oligocene  
477 (from ca 33.2Ma). At Site 748, the fine fraction  $\delta^{13}\text{C}$  curve shows less fluctuation than the benthic curves during the  
478 middle Late Eocene. A synchronous  $\delta^{13}\text{C}$  increase (ca 0.6‰ shift) is observed at 36.5 Ma. Elevated fine fraction  $\delta^{13}\text{C}$   
479 values are observed from the late Eocene until the early Oligocene, coherent with previous studies (Bohaty et al., 2003),  
480 while the benthic values stay low during the same period (Figure 3D and F).

481 ~~Our new oxygen (Figure 3C and E) and carbon (Figure 3D and F) stable isotope data allow us to identify previously~~  
482 ~~noted trends and distinct events during the period studied. Benthic  $\delta^{18}\text{O}$  values exhibit an overall increasing trend during~~  
483 ~~the late Eocene indicating the overall decrease of oceanic bottom water temperatures. A sharp increase occurs at the~~  
484 ~~Eocene-Oligocene transition (between 33.9 and 33.3 Ma) in both sites examined. This rapid shift has been observed in~~  
485 ~~several sites in the Southern Ocean (e.g., Muza et al., 1983; Miller et al., 1987; Mackensen and Ehrmann, 1992; Zachos~~



486 et al., 1996; Billups et al., 2002; Pusz et al., 2011) and it is well established as a global signal (Zachos et al., 2001). It is  
487 generally interpreted as a combination of deep ocean water cooling and major ice growth on the Antarctic continent  
488 (Zachos et al., 2001). At Site 689, the planktic  $\delta^{18}\text{O}$  curve almost mimics the benthic one. The  $\delta^{18}\text{O}$  values measured on  
489 fine fraction reveal a heavier trend more pronounced at ODP Site 748 (Kerguelen Plateau) compared to ODP Site 689  
490 (Maud Rise). During the Eocene, heavier values are observed around 37 Ma in both Atlantic and Indian Sectors of SO.  
491 Both benthic and planktic foraminifera  $\delta^{13}\text{C}$  records show fluctuations across the period studied, with low values across  
492 the Eocene-Oligocene boundary, followed by an increase that accompanied the  $\delta^{18}\text{O}$  increase and low values again in  
493 the upper Oligocene. The benthic trend is also observed by previous data from the same sites (Mackensen and Ehrmann,  
494 2002; Diester-Haass and Zahn, 1996; Bohaty et al., 2003). The fine fraction records show elevated  $\delta^{13}\text{C}$  values between  
495 Late Eocene to Early Oligocene, followed by a decreasing trend during the Oligocene (from ca 33.2Ma). At Site 748,  
496 the fine fraction  $\delta^{13}\text{C}$  curve shows less fluctuation than the benthic curves during the middle Late Eocene. A  
497 synchronous  $\delta^{13}\text{C}$  increase (ca 0.6‰ shift) is observed at 36.5 Ma. Elevated fine fraction  $\delta^{13}\text{C}$  values are observed from  
498 the late Eocene until the early Oligocene, coherent with previous studies (Bohaty et al., 2003), while the benthic values  
499 stay low during the same period (Figure 3D and F).

### 500 | 3.3 $p\text{CO}_2$ Proxies

501 As noted above, given the complexities and potential biases of compiling data from different proxies and different time  
502 intervals, we prefer to use the single site single proxy time series of  $p\text{CO}_2$  from Zhang et al. (2013). This data (Figure 4)  
503 shows two peaks in the late Eocene, with a maximum for the entire study interval at ca 37 Ma and a smaller peak at ca  
504 34.5 Ma, and a rapid drop of over 200 ppm from nearly 1000 to ca 750 ppm in the earliest Oligocene (ca 33.5 Ma).  
505 Despite the limitations of multi-proxy, multi-site compilations, the compiled data (Table S2; Figure S7) shows the same  
506 basic features, nor does the result appear to be sensitive to the precise choice of data to include in the analysis.

## 507 | 4 Discussion

### 508 | 4.1 Correlation of Productivity to Ocean Circulation, Glaciation and $p\text{CO}_2$ Change

509 Intervals of high export productivity (bio-Ba) exhibit synchronous changes with intervals of changes in oxygen and  
510 carbon stable isotopes and  $p\text{CO}_2$  data (Figures 3 and 4). Notably, these intervals occur in the late-Eocene (~ 37 Ma) and  
511 at the E/O boundary (~34 Ma). This correlation is highly suggestive that ocean circulation, glaciation, productivity and  
512 atmospheric  $p\text{CO}_2$  changes are interconnected. It could be assumed that (1) primary processes, such as ocean circulation  
513 and glaciation are independently driving productivity and  $p\text{CO}_2$  changes, or (2) a cascading effect, with glaciation and  
514 ocean circulation influencing productivity and, consequently, altering atmospheric  $p\text{CO}_2$  levels. While we cannot in our  
515 study distinguish between these two possibilities, we explore the second, as proposed by Egan et al. (2013), in which  
516 changes in ocean conditions due to tectonic-climate drivers affect productivity, and the latter in turn  $p\text{CO}_2$  levels.

## 517 | 4 Discussion

### 518 | 4.2 Late Eocene Productivity Event and its Potential Impact

519 | The noticeable bio-Ba AR peak at ~ 36.8 Ma (Figure 2), suggests an important, ca 1 ~~M~~my long event of approximate  
520 doubling of export productivity during the late Eocene, preceding the significant cooling and the first formation of large  
521 Antarctic ice sheets at the Eocene-Oligocene boundary. The temporal synchronicity among different site locations in the  
522 Southern Ocean suggests that the process driving this enhanced export productivity in the late Eocene occurred  
523 throughout the Southern Ocean, requiring a mechanism that increased the delivery of nutrients to the surface ocean.  
524 | Our findings corroborate previous ~~\_, more limited~~ paleoproductivity studies that indicate an increase in export  
525 productivity in the Atlantic Sector of the Southern Ocean during this time period. Anderson and Delaney (2005) found  
526 several peaks in productivity indicators at the Agulhas Ridge during the same time interval, and benthic foraminiferal  
527 accumulation rates show an increase in paleo-primary productivity on Maud Rise (Diester-Haass & Faul, 2019) (Figure  
528 2). A pronounced opal abundance peak is also documented by Diekman et al. (2004) between 37.5 and 33.5 Ma at the  
529 ODP Site 1090. ~~The Kerguelen productivity record from Site 744 data shows a substantial peak around 37 Ma and an~~  
530 ~~earlier one near 40 Ma.~~ Our results ~~now sthus~~ show that the 37 Ma event extended at least as far as the Kerguelen  
531 Plateau in the Indian Ocean sector, ~~with a substantial peak around 37 Ma and an earlier one near 40 Ma~~, thus affecting a  
532 ~~large portion~~most of the Southern Ocean region.  
533 | A direct analysis of the impact of the potential significance of this event for the development of late Eocene global  
534 climate depends on two key factors: the extent to which the increased productivity contributed to enhanced carbon  
535 sequestration, and the magnitude of sequestration over the ca 1 my interval of enhancement. Understanding the impact  
536 of productivity on carbon sequestration for the Eocene oceans however is complicated by the lack of knowledge of  
537 several factors that influence this process. These factors include our ability to estimate the impact of higher productivity  
538 on carbon sequestration is limited, as many of the factors that affect this in the modern ocean are poorly understood for  
539 Eocene oceans (export efficiency to the subsurface waters, rates of transport and degradation in the water column and  
540 upper sediment layers, organic carbon content of Southern Ocean Eocene pelagic sediments; as well as transport of  
541 organic carbon by subsurface water layers in the late Eocene oceans to lower latitude areas of productivity and  
542 sequestration. We therefore cannot directly calculate the impact that the observed productivity change had on pCO<sub>2</sub>.  
543 Instead we take an indirect approach, comparing the productivity history to the history of pCO<sub>2</sub> and potential drivers of  
544 productivity change such as ocean circulation and climate change.

#### 545 | 4.3 Surface Water Changes in Physical Conditions in the Late Eocene

546 | ~~The potential significance of this event for the development of late Eocene global climate depends on the extent to~~  
547 ~~which the enhanced productivity contributed to enhanced carbon sequestration, and the magnitude of sequestration over~~  
548 ~~the ca 1 my interval of enhancement. Our ability to estimate the impact of higher productivity on carbon sequestration is~~  
549 ~~limited, as many of the factors that affect this in the modern ocean are poorly understood for Eocene oceans (export~~  
550 ~~efficiency to the subsurface waters, rates of transport and degradation in the water column and upper sediment layers;~~  
551 ~~organic carbon content of Southern Ocean Eocene pelagic sediments; as well as transport of organic carbon by~~  
552 ~~subsurface water layers in the late Eocene oceans to lower latitude areas of productivity and sequestration). For~~  
553 ~~simplicity we thus use values for the modern Southern Ocean, but conservatively ignore the (in the modern oceans)~~  
554 ~~substantial transport of nutrients in the modern ocean to lower latitudes by Antarctic Intermediate Water (Sarmiento et~~  
555 ~~al., 2004). The purpose of such a calculation is simply estimating if the magnitude of enhanced productivity, could,~~  
556 ~~within the region studied, and over the 1 my interval of the event, at least potentially have sequestered a climatically~~

557 significant amount of carbon. Using Hayes et al. (2021) data on the composition and flux of seafloor sediments in the  
 558 Global Ocean, we compute the mean total organic carbon (TOC) exported to deep-sea sediments per cm<sup>2</sup> per year in the  
 559 Southern Ocean (SO, area below the polar front and above the Antarctic continent), the Polar Frontal Zone (PFZ, based  
 560 on Park et al. 2019 coordinates for the subantarctic and polar fronts) and, as a subset of the SO total, just the Atlantic  
 561 sector of the Southern Ocean. We thus estimate the total amount of organic carbon currently exported to the deep sea  
 562 per year in these areas. Finally, given the approximate doubling of productivity during the 1 my interval, we compute  
 563 the amount of excess exported carbon over 1 Myr, and translate it into the corresponding amount of atmospheric CO<sub>2</sub> in  
 564 ppm (using Clark 1982 equivalency) to roughly estimate the order of magnitude of how much carbon the biological  
 565 carbon pump could have buried in the sediments of the area of interest. The results (Table 2) suggest that enhanced  
 566 carbon sequestration in the late Eocene SO, even if restricted only to the Atlantic sector, could have indeed been  
 567 sufficient to have affected global pCO<sub>2</sub> (hypothesis 2 as stated in the introduction). If the enhanced productivity affected  
 568 most, or all of the circumpolar region, and if indirect carbon sequestration via intermediate water transport also played a  
 569 role the impact could have been dramatic.

570 **Table 2.** Potential impact of doubling modern Southern Ocean export productivity/carbon sequestration for a 1 my time  
 571 interval. See text for definitions of areas and calculations.

Region	Area (km <sup>2</sup> )	Mean TOC (gC cm <sup>-2</sup> yr <sup>-1</sup> )	Exported carbon (PgC Myr <sup>-1</sup> )	Equivalent pCO <sub>2</sub> (ppm)
Southern Ocean	35 882 985	0.004882	1 751.856	882.5
PFZ	10 290 123	0.004326	445.108	209.0
Atlantic Sector of SO	11 561 803	0.005047	583.518	274.0

#### 572 4.2 Surface Water Changes in Physical Conditions in the Late Eocene

573 The late Eocene is generally accepted as a time interval of gradual cooling of Southern Ocean waters. Indeed,  
 574 biomarker-based temperature estimates reveal substantial (3-5 °C) high latitude sea surface temperatures (SST) cooling  
 575 within the late Eocene (Liu et al., 2009; O'Brien et al., 2020). Our fine fraction stable oxygen isotopes confirm this  
 576 cooling trend following MECO, with a distinct peak at 37 Ma during the Eocene, matching the peak cooling reported by  
 577 O'Brien et al. (2020). This interval of maximum δ<sup>18</sup>O values occurred during the same interval in which export  
 578 productivity increased (Figure 2). In this interval the difference in the δ<sup>18</sup>O gradient between benthic foraminifera and  
 579 fine fraction (nannofossil) carbonate is less pronounced. This increase in similarity is interpreted as having been  
 580 either be caused by a decrease in water column stratification and or by enhanced vertical mixing. In other words, either  
 581 the (temperature) conditions during deposition were identical across larger areas and depths, or water masses were  
 582 mixed more frequently.

583 This change in export productivity in the late Eocene is coeval with a change towards increasing variability of carbon  
 584 stable isotopes (δ<sup>13</sup>C) of benthic foraminifera (Figure 4). Although δ<sup>13</sup>C in individual sections can also represent local  
 585 effects, usually there is a strong component of global changes in carbon reservoirs, and indeed our local measurements  
 586 closely align with the global curve (Figure 3B, D and F). In the global context, a shift towards more positive values in  
 587 the benthic δ<sup>13</sup>C at ~ 37 Ma indicates a carbon cycle perturbation. This shift coincides with the export productivity  
 588 changes observed in our study. One possible explanation is that higher productivity may have elevated the export flux of

589 | organic carbon to sediments, thereby increasing the marine organic carbon burial and preferentially scavenging the  
590 | lighter  $^{12}\text{C}$  from the carbon pool.

591 | ~~This change in export productivity in the late Eocene is coeval with a change towards increasing variability carbon~~  
592 | ~~stable isotopes ( $\delta^{13}\text{C}$ ) of benthic foraminifera (Figure 4). Benthic foraminiferal  $\delta^{13}\text{C}$  provides a powerful tracer for the~~  
593 | ~~reconstruction of bottom water circulation patterns, nonetheless, should be carefully interpreted because the signal can~~  
594 | ~~be overprinted by multiple effects such as the global carbon cycle or local dissolved nutrient contents. Comparing our~~  
595 | ~~local stable carbon isotope records to a global compilation shows that the local  $\delta^{13}\text{C}$  curves fit reasonably well within~~  
596 | ~~the global records (Figure 3B, D and F). In the global context, a shift towards more positive values in the  $\delta^{13}\text{C}$  at 37 Ma~~  
597 | ~~demonstrates a carbon cycle perturbation. The subsequent decrease towards more positive values in the late-Eocene is~~  
598 | ~~coeval with the global trend and also coincides with the productivity changes. One possible explanation is that the~~  
599 | ~~marine organic carbon burial is increased, preferentially scavenging the light  $^{12}\text{C}$  from the carbon pool.~~

600 | ~~This adds evidence to an event of high productivity during the late Eocene. However, in the Indian Sector and~~  
601 | ~~afterwards in the Atlantic Sector of the Southern paleo-Ocean, the local  $\delta^{13}\text{C}$  does not follow the secular trend. This~~  
602 | ~~argues that ocean circulation also changes along with productivity.~~

#### 603 | **4.43 Oceanographic Circulation Drivers of the Late Eocene Productivity Change**

604 | We propose that the main cause for the productivity increase observed in the late Eocene is the upwelling of nutrient-  
605 | rich deep waters. Understanding however the physical oceanographic mechanisms that led to increased upwelling  
606 | throughout the Southern Ocean requires examining links between the different processes that occurred at that time  
607 | period. Changes in paleoceanography during the Paleogene were significantly mediated through tectonic re-  
608 | organisation, such as the Southern Ocean gateways opening (i.e., the Drake Passage and the Tasman Gateway), changes  
609 | in the Atlantic-Arctic gateway and in the Tethys Seaway.

610 | In this context, the Southern Ocean circulation during this time period is still debated due to uncertainties concerning  
611 | the opening of the gateways that led to the development of the Antarctic Circumpolar Current (ACC). Estimates for the  
612 | onset of the modern-like ACC have not reached a consensus yet and vary from as early as middle Eocene (ca 41 Ma,  
613 | Scher & Martin, 2006; ca 35.5 Ma, Stickley et al. 2004) to middle Oligocene (ca 23Ma; Pfuhl and McCave, 2005). This  
614 | inconsistency suggests that the onset of ACC could have been a gradual or an intermittent change. Further, local proxy  
615 | records cannot distinguish between regionally developed fronts and true circumpolar flow (i.e. ACC).

616 | ~~In this context, the Southern Ocean circulation during this time period is still debated due to uncertainties concerning~~  
617 | ~~the opening of the gateways that led to the development of the Antarctic Circumpolar Current (ACC). Estimates for the~~  
618 | ~~onset of the modern-like ACC have not reached a consensus yet and vary from as early as middle Eocene (ca 41 Ma,~~  
619 | ~~Scher & Martin, 2006; ca 35.5 Ma, Stickley et al. 2004) to middle Oligocene (ca 23Ma; Pfuhl and McCave, 2005). This~~  
620 | ~~inconsistency suggests that the onset of ACC could have been a gradual or an intermittent change. Further, local proxy~~  
621 | ~~records cannot distinguish between regionally developed fronts and true circumpolar, i.e. ACC flow.~~

622 | In addition to  $\delta^{18}\text{O}$  and  $\delta^{13}\text{C}$ ,  $\epsilon\text{Nd}$  has been used to identify circulation changes and water masses exchange through the  
623 | Eocene (Scher and Martin, 2004, 2008; Scher et al., 2014; Huck et al., 2017; Wright et al., 2018). Nd isotopes are one of  
624 | the most robust tracers of water mass origin (Frank, 2002). The residence time of Nd in oceans is much shorter (300--

625 1000 years) than ocean mixing time and is thus distinct at a given location. Further, the isotope composition of the Nd  
626 ocean budget is solely determined by terrigenous contribution. The latter is balanced by Nd sinks that remove Nd  
627 quantitatively, yet this only influences the net budget and thus the magnitude and/or swiftness of changes to the  $\epsilon_{\text{Nd}}$   
628 composition. However, mixing of water masses, e.g. through lateral or vertical mixing, can also cause changes as long  
629 as they occur more rapidly than the residence times.

630 In the late Eocene, starting at 37 Ma, Scher and Martin (2004) found a dramatic positive shift in  $\epsilon_{\text{Nd}}$  values in the  
631 Atlantic sector of the SO that they interpreted as the influx of Pacific deep waters, due to its characteristic of more  
632 radiogenic (positive) waters, not previously observed in the Atlantic Ocean. Recently published Nd isotope records from  
633 the Kerguelen Plateau (Wright et al., 2018) revealed a long-term negative trend during the late Eocene, which also  
634 suggests that the water mass mixing between the Pacific and Atlantic preceded 36 Ma.  $\epsilon_{\text{Nd}}(t)$  records from the  
635 Kerguelen Plateau in fact showed values comparable to modern CDW during the Oligocene, inferring water mass  
636 composition similar to the present day. Thus, Nd isotope data support at least partial opening of Drake Passage by the  
637 late Eocene (before 36 Ma), consistent with plate tectonic reconstructions (Livermore et al., 2005, 2007). Regardless of  
638 the depth, Neodymium isotope evidence for late Eocene opening of the Drake Passage suggests that increased fetch for  
639 surface flow and changing deep water composition could have had changes in the surface water conditions in the South  
640 Atlantic sector of the late Eocene Southern Ocean.

641 This has been explicitly demonstrated in a recent modelling study conducted by Toumoulin et al. (2020). They  
642 demonstrate that the Drake Passage opening, even at shallow depth, notably connects prior regional frontal systems  
643 together, thereby allowing the formation of a proto-ACC; and has a strong effect on the Southern Ocean Eocene water  
644 mass structure, inducing ocean cooling in most of the Southern Hemisphere. These temperature changes are not linear  
645 and differ from one region to another, with DP opening causing changes in the mixed layer depths and provoking  
646 different responses in the Atlantic and Indian Sectors of the SO. In the Atlantic and Indian Ocean sectors in particular,  
647 very deep seasonal mixing (several hundred meters) over broad areas of the entire region is replaced by more moderate  
648 levels of mixing (generally ca 200 m or less), except near the proto-polar front region, where seasonal mixing of 300-  
649 400 m still occurs. Vila et al. 2014 have found nannofossil assemblages characteristic of cool sea surface waters in the  
650 late-Eocene in Kerguelen Plateau samples. Cooler temperatures are coeval with the paleoceanographic re-organization  
651 and intensified upwelling that we infer for this time period, while differences in the depth of the mixed layers between  
652 ocean basins may explain the different magnitude of export productivity observed in the Atlantic and Indian sectors of  
653 the SO.

654 The wind-driven eastward flow and the characteristic fronts of the modern ACC support the upwelling of nutrient-rich  
655 water to the surface and consequently high levels of productivity. On the balance of evidence, it seems that the export  
656 productivity seen in our data in the late Eocene is likely to have occurred in response to a proto-ACC front's  
657 development and its associated upwelling. The inferred onset of a proto-ACC in the late Eocene and our finding of  
658 increased upwelling fits the hypothesis that ACC type circulation itself helps drive the AMOC circulation (Toggweiler  
659 and Bjornsson, 2000; Katz et al., 2011; Sarkar et al., 2019). A proto-ACC causes SO upwelling, and thus provides  
660 support for increasing AMOC-like circulation in the late Eocene as an additional cause of increased upwelling as a  
661 causative mechanism of the export productivity event. Temperature asymmetry between Northern and Southern  
662 Hemisphere and comparisons between benthic  $\delta^{13}\text{C}$  records provide evidence for the strengthening of the AMOC in the  
663 late Eocene (Elsworth et al., 2017).



#### 664 | 4.54 Eocene-Oligocene Boundary Productivity Changes

665 | The earliest Oligocene, following the E/O boundary ~~OF~~, has been suggested as a period of a significant rise in biological  
666 | productivity in high southern latitudes (Diester-Haass, 1995, 1996; Diester-Haass and Zahn, 1996, 2001). However, in  
667 | contrast to the late Eocene event, the export productivity changes across the Eocene-Oligocene boundary observed in  
668 | our study were not always concurrent between the sites investigated (Figure 2). In the Atlantic sites, export productivity  
669 | increases and decreases several times from the late Eocene to early Oligocene. We thus argue that the fluctuations in  
670 | export productivity that occurred in the Southern Ocean during this global climatic re-organization are more strongly  
671 | modulated by local parameters, whereas the late Eocene productivity event is more uniform and reflects the global re-  
672 | organization of ocean circulation. If the trends observed in export productivity across the EOT were regulated only by  
673 | global, or at least regional temperature and circulation changes, then we would observe significant changes also in the  
674 | Indian sector of the Southern Ocean. It seems however that productivity increase was more pronounced in the Atlantic  
675 | sector of the Southern Ocean.

676 | Today, the Southern Ocean (SO) has a frontal system that strongly impacts circulation, primary productivity and the  
677 | entire climate system (Chapman et al., 2020). The Antarctic Polar Front (APF) is particularly important for controlling  
678 | nutrient distribution. Latitudinal variations of the APF for example have been shown to alter regional productivity over  
679 | the glacial cycles (Kim et al., 2014, Thole et al., 2019). The causes of the lack of significant export productivity changes  
680 | in the Indian sector of the Southern Ocean during the early Oligocene after the Eocene-Oligocene boundary are unclear.  
681 | The Kerguelen Plateau may not have been located in a position favourable to nutrient-rich upwelling. In addition, the  
682 | regional frontal migration may have been more intense in the Atlantic sector compared to the Indian sector of the SO.

#### 683 | 4.65 A Scenario for Southern Ocean Productivity and Circulation Change in the Late Eocene

684 | The patterns of productivity change seen in our study can be placed in an (admittedly speculative) scenario, which is at  
685 | least compatible with prior studies and modelling of conditions in the late Eocene austral ocean region and Antarctica.  
686 | In the earliest interval covered in our study (ca 40-38 Ma) productivity was in most sites fairly low (Figure 5a). At this  
687 | time there is little evidence for a significant influx of Pacific waters into the Atlantic, and the Drake Passage is thus  
688 | assumed to be effectively closed to ocean circulation.

689 | During the 38-36 Ma interval, evidence summarised by Scher et al. (2014) suggests that a significant, if transient,  
690 | glaciation event occurred on the Antarctic continent—the Priabonian oxygen maximum, or PriOM. If sufficient in  
691 | magnitude this would have significantly affected circulation throughout the austral ocean region, with strengthened  
692 | temperature gradients, ~~invigorated stronger~~ circumpolar circulation (Houben et al., 2019), and increased upwelling  
693 | (Goldner et al, 2014). This would account both for the substantial increase in productivity, and the broad geographic  
694 | extent of the increase seen in our data (Figure 5b). The cause of this glaciation event is unknown, but may be related in  
695 | part to the trend in the late Eocene towards lower atmospheric  $p\text{CO}_2$  interacting with orbital fluctuations in polar  
696 | insulation as explored in model simulations by Van Breedam et al. (2022).

697 | With the end of transient glaciation, the atmospheric forcing of ocean circulation would have declined, and with it the  
698 | high levels of productivity seen in our data (Figure 5c). However, by this time (ca 36-34 Ma) the Nd isotope data  
699 | suggests that a significant influx of Pacific water was reaching the South Atlantic sector of the austral ocean (Scher and  
700 | Martin, 2004), and consequently, the Drake Passage must have been at least partially open. This would have resulted in,  
701 | if not as strong as during the PriOM, nonetheless stronger circumpolar circulation in a proto-ACC, increased upwelling,

702 and increased nutrient availability from Pacific-sourced deep waters. The locus of high productivity would have become  
703 however more cantered near the proto-ACC, which at that time, according to the model results of Toumoulin et al.  
704 (2020) was located a few degrees north of the current location of the ACC. The high productivity and accumulation of  
705 biogenic opal seen at Site 1090, fortuitously located at this time in this region can be thus be explained, as can the lower  
706 relative productivity of Site 689, located much further to the south and thus outside the region primarily influenced by  
707 the proto-ACC system.

708 Lastly, at the E/O boundary itself (Figure 5d), the well known major shifts in oxygen isotopes signal the formation of a  
709 full continental ice-sheet, which would have in turn driven a renewed increase in circumpolar ocean circulation- a full,  
710 if early form of the ACC, and dramatically increased levels of productivity, again however primarily near the ACC  
711 region.

#### 712 | 4.76 Possible Implications to the EOT Global Cooling

713 Our  $p\text{CO}_2$  compilation shows that carbon dioxide levels declined gradually from ca 1200 ppm in the late Eocene to ca  
714 750 ppm across the EOT (Figure 4 and Figure S7). There are different processes involved in the oceanic uptake of  $\text{CO}_2$ .  
715 The solubility pump is a physical-chemical process that promotes gas transfer between the atmosphere and sea-water in  
716 order to achieve chemical equilibrium. This process depends on temperature, in which the solubility increases as  
717 temperature decreases. Evidence for cooling of surface waters observed in the Southern Ocean (Liu et al., 2009;  
718 Hutchinson et al., 2021) could have favoured the ability to dissolve atmospheric  $\text{CO}_2$ , ~~thus being an important~~  
719 ~~contributor~~ to the drawdown of  $p\text{CO}_2$  during the late-Eocene.

720 Silicate weathering has been suggested to play an essential role in regulating  $\text{CO}_2$  across the EOT (Zachos and Kump,  
721 2005). On geologic time scales, chemical silicate weathering is considered to modulate atmospheric  $\text{CO}_2$  levels through  
722 a negative feedback mechanism (Berner et al., 1983). Weathering of silicate rocks provides a source of alkalinity to  
723 the oceans, acting as a sink for atmospheric  $\text{CO}_2$ , thereby influencing global climate. In addition, increasing  
724 silicate weathering enhances primary productivity through the delivery of nutrients to the ocean. Intensified  
725 weathering is supported by Os isotope records, showing an anomaly before the EOT, at ca 35.5Ma (Dalai et al., 2006).

726 High export productivity potentially modulates  $\text{CO}_2$  by two major mechanisms, operating over very different time  
727 scales. Productivity maintains a gradient in dissolved  $\text{CO}_2$  between the surface and deep ocean by exporting organic  
728 carbon from the surface into deep ocean waters. This in turn lowers the concentration of  $\text{CO}_2$  in surface waters, causing  
729 more atmospheric  $\text{CO}_2$  to be drawn out of the atmosphere into dissolved surface ocean  $\text{CO}_2$ . It is estimated that this  
730 mechanism causes  $p\text{CO}_2$  to be approximately 200 ppm lower than it would in a purely abiotic ocean (Volk and Hoffert  
731 1985). In the second mechanism, in areas of the ocean with high export productivity a (generally rather small) fraction  
732 of biologically captured carbon (both soft tissue and carbonate from coccolithophores and planktic foraminifera)  
733 escapes remineralization in the water column and is buried in ocean bottom sediments, where it is sequestered for  
734 (typically) many millions of years. Changes in either mechanism can contribute to the decline of atmospheric carbon  
735 dioxide, thereby intensifying the cooling trend. Therefore, the observed increase in export productivity in the late-  
736 Eocene over 1 My in multiple sites in the SO, and the temporal correlation with the changes in  $p\text{CO}_2$  proxy records  
737 showed in our study is compatible with the hypothesis proposed by Egan et al., 2013. This suggests that the heightened  
738 export productivity identifying in our study is a potential candidate that may have provided important positive feedback  
739 to the  $p\text{CO}_2$  decline.

740 However, this correlation is suggestive rather than conclusive, given the complexities of the carbon cycle. For instance,  
741 variations in the efficiency of the carbon pump, remineralization (Griffith et al., 2021), the relationship between  
742 nutrients availability and plankton utilization and the dynamics of shelf-deep sea carbonate (Sluijs et al., 2013) can  
743 significantly influence the relationship between export productivity and  $p\text{CO}_2$  levels and adds complexity to our  
744 understanding. Limited data for the late-Eocene on some critical parameters to our understanding (e.g. sedimentary  $\text{C}_{\text{org}}$ ,  
745 Olivarez Lyle & Lyle, 2006) further contributes to the uncertainties in establishing a causal link. Moreover, it is  
746 essential to note that upwelling, while promoting nutrient-rich conditions favourable to productivity and the long-term  
747 sequestration mechanism, also contribute to outgassing of  $\text{CO}_2$  into atmosphere, influencing the carbon balance in the  
748 short-term mechanism. This adds another layer of complexity to the carbon cycle dynamics and its relationship with  
749 productivity changes. While our findings propose a potential link, it is crucial to recognize that this alone does not  
750 constitute proof of the export productivity directly influenced late Eocene  $p\text{CO}_2$  levels.

751 ~~The potential effects of enhanced export productivity could have modulated these changes in  $\text{CO}_2$  because it removes~~  
752 ~~organic carbon from the surface ocean and transport it into the deep ocean, and thus via sequestration is a mechanism~~  
753 ~~that contributes to the decline of atmospheric carbon dioxide and intensifies the cooling trend. Therefore, enhanced~~  
754 ~~productivity in the late-Eocene and at Eocene-Oligocene transition recorded in our study is a potential candidate that~~  
755 ~~may have provided important positive feedback to the  $p\text{CO}_2$  decline.~~

756 Despite some modelling studies showing that circulation changes were not the main factor in driving the cooling and  
757 glaciation on Antarctica (e.g. Huber et al., 2004; Huber and Not 2006; Sijp et al., 2011), circulation changes still had a  
758 significant impact, with e.g. Southern Ocean sea surface temperature declines of 2-4°C (Toumoulin et al., 2020),  
759 ~~increased~~ affecting the atmosphere-ocean  $\text{CO}_2$  equilibrium. A succession of events may have contributed to the evolution  
760 of climate: thermal isolation of Antarctica, glaciers formation, increasing intensity of silicate weathering, together with  
761 upwelling of nutrient rich and cold deep waters, leading to ~~higher solubility pump and~~ high biological productivity, then  
762 declining  $p\text{CO}_2$ . Moreover, because the Atlantic Meridional Overturning Circulation (AMOC) affects the distribution of  
763 tracers such as temperature, dissolved inorganic carbon (DIC), alkalinity and nutrients (Boot et al., 2021), the  
764 strengthening of AMOC could explain the further decrease in atmospheric  $\text{CO}_2$  via biological export productivity.  
765 Elsworth et al., (2017), for example, suggest that enhanced weathering is driven by intensified AMOC in the latest  
766 Eocene due to increasing AMOC causing differential global distribution and increase of surface temperatures and  
767 precipitation over land areas. These factors together suggest that E-O changes in AMOC also may play an important  
768 role as a driver of  $\text{CO}_2$  decline.

769 Taken together, the above processes indicate that a variety of positive feedbacks contributed to Antarctic glaciation from  
770 about 37 Ma onwards. Recent evidence suggests that continental-scale Antarctic glaciation initiated in the late Eocene  
771 (Scher et al., 2014; Carter et al., 2017). Our results indicate that significant changes in Southern Ocean export  
772 productivity preceded the E/O boundary by approximately 3 million years. These trends are likely to be a response to  
773 the combination of the intensified processes that had been in place since the late Eocene. The correlation between our  
774 Southern Ocean productivity peaks and decline in global  $p\text{CO}_2$  records, and suggest that biological productivity may  
775 have played an important role in the drawdown of  $p\text{CO}_2$  levels. Specifically enhanced ~~The~~  $\text{CO}_2$  fixation by  
776 phytoplankton and carbon ~~sequestration in export to the seafloor~~ ~~sediments increased~~ ~~increased~~ via an increase in the  
777 biological pump may have contributed to decrease atmospheric  $\text{CO}_2$ , ~~and~~ through a positive feedback from declining  
778 Southern Ocean surface water temperature enhanced boosting ~~and, thus boosting~~ the cooling trend. The establishment  
779 of Antarctic glaciation may thus have been influenced significantly by enhanced productivity. ~~What remains unclear is~~

780 | ~~the biological drivers (plankton) of this productivity change and their role in the long-term evolution of global climate~~  
781 | ~~change.~~

## 782 | **4.87 Limitations and Future Directions**

783 | Our study has numerous limitations. Our data on paleoproductivity does not cover the full time interval in all of the sites  
784 | studied, and our geographic coverage is still incomplete. In particular, we have not examined sections from the Pacific  
785 | sector, or the influence of the Tasman gateway. Most of our interpretations are based on a single productivity proxy -  
786 | biogenic Barium. While this proxy is well established and gives coherent results in our study, productivity proxies are  
787 | known to have complex behaviours, and results using different proxies might be at least somewhat different. Our  
788 | ~~suggestion that estimates of how much~~ elevated late Eocene Southern Ocean productivity might have affected global  
789 | carbon sequestration is only a ~~speculation based on general characteristics of the ocean carbon system, and rough~~  
790 | ~~estimate of potential magnitude and~~ much more detailed study of both actual sequestration values in sediment, and the  
791 | impact on atmospheric  $p\text{CO}_2$  are still needed. Our interpretative scenario attributing productivity changes to a  
792 | combination of Drake Passage opening and continental scale glaciation on Antarctica are ~~also~~ purely qualitative and  
793 | need further study. Despite these limitations, our study sheds new light on the late Eocene oceanic precursors of the  
794 | Eocene-Oligocene glaciation event—the most dramatic climate change of the Cenozoic.

## 795 | **5 Conclusions**

796 | Our bio-Ba data provide important records of the Southern Ocean productivity history across the EOT. These data show  
797 | that export productivity increased significantly in the late Eocene in the Southern Ocean and was affected by ocean  
798 | circulation changes. The development of a regionally varying circumpolar polar flow (proto-ACC) and the associated  
799 | frontal system ~~proposed by other recent studies~~ is likely to have contributed to the enhanced productivity in the  
800 | Southern Ocean through the intensification of upwelling (H1).

801 | Our results show that increasing Southern Ocean productivity in the late Eocene to earliest Oligocene is correlated to  
802 | global changes in atmospheric  $p\text{CO}_2$  and carbon isotope proxies for organic carbon extraction. This finding points  
803 | toward a potential positive climate system feedback, involving ocean circulation changes, enhanced export productivity  
804 | and drawdown of atmospheric  $\text{CO}_2$ . Although ~~many studies of the Eocene-Oligocene climate transition try to identify a~~  
805 | ~~single have the inclination to point to a~~ dominant mechanism (e.g. ocean gateway opening vs  $p\text{CO}_2$  decline) for causing  
806 | the initiation of Antarctica glaciation, each mechanism plays a different role and has associated complex feedbacks.  
807 | Our study points toward a climate feedback system involving ocean circulation, thermal isolation and biological  
808 | productivity, where several mechanisms are interconnected and cannot be considered separately. Openings of gateways  
809 | led to the development of a circumpolar flow, promoting cooling and increased upwelling that contributed to ~~enhanced~~  
810 | ocean carbon pump ~~activity s~~ and ~~promotes~~ the decline of atmospheric carbon dioxide.

## 811 | **Data Availability**

812 | The supplementary information related to this article is available in the Supplement, the raw data will be available upon  
813 | publication in an open-access database (PANGAEA: <https://www.pangaea.de>).

## 814 | **Author Contributions**

815 The manuscript was designed and written by GRF in collaboration with DL. DL updated age models. GRF prepared all  
816 the samples for geochemical analyses. JS ~~ran the~~ barium and aluminum analyses. US generated carbon and oxygen  
817 stable isotope data.  $p\text{CO}_2$  data and neodymium isotopes data were compiled by GRF. Biogenic barium was calculated  
818 by GRF. All authors contributed to editing the manuscript.

## 819 Competing Interests

820 The authors declare that they have no conflict of interest.

## 821 Acknowledgments

822 This study was funded by the Federal Ministry of Education and Research (BMBF) under the “Make our Planet Great  
823 Again, German Research Initiative”, grant number 57429681, implemented by the German Academic Exchange Service  
824 (DAAD).

## 825 References

- 826 Anagnostou, E., John, E. H., Edgar, K. M., Foster, G. L., Ridgwell, A., Inglis, G. N., Pancost, R. D., Lunt, D. J., and  
827 Pearson, P. N. Changing atmospheric CO<sub>2</sub> concentration was the primary driver of early Cenozoic climate. *Nature*,  
828 v. 533, pp. 380-384. <https://doi.org/10.1038/nature17423>, 2016.
- 829 Anagnostou, E., John, E. H., Babila, T.L., Sexton, P. F., Ridgwell, A., Lunt, D.J., Pearson, P.N., Chalk, T.B., Pancost,  
830 R.D. and Foster, G.L. Proxy evidence for state-dependence of climate sensitivity in the Eocene greenhouse. *Nature*  
831 *Communications*, 11, 4436 (2020). <https://doi.org/10.1038/s41467-020-17887-x>, 2020.
- 832 Anderson, L.D. & Delaney, M.L. Middle Eocene to early Oligocene paleoceanography from Agulhas Ridge, Southern  
833 Ocean (Ocean Drilling Program Leg 177, Site 1090). *Paleoceanography and Paleoclimatology*, 20, 1.  
834 <https://doi.org/10.1029/2004PA001043>, 2005.
- 835 Anderson, J.B., Warny, S., R.A. Askin, J.S. Wellner, S.M. Bohaty, A.E. Kirshner, D.N. Livsey, A.R. Simms, T.R. Smith,  
836 W. Ehrmann, L.A. Lawver, D. Barbeau, S.W. Wise, D.K. Kulhanek, F.M. Weaver, W. Majewski. Progressive  
837 Cenozoic cooling and the demise of Antarctica's last refugium, *PNAS*, 108, pp. 11356-11360, 2011.
- 838 [Archer, D., Winguth, A., Lea, D., Mahowald, N. What caused the glacial/interglacial atmospheric  \$p\text{CO}\_2\$  cycles? \*Reviews\*  
839 \*of Geophysics\*, 38 \(2\), 159-189. <https://doi.org/10.1029/1999RG000066>, 2000.](https://doi.org/10.1029/1999RG000066)
- 840 Arrhenius, S. On the influence of carbonic acid in the air upon the temperature of the ground. *Philosophical Magazine*  
841 *and Journal of Science*, 5, v.41, 237-276, 1986.
- 842 Aubry, M.P. Late Paleogene Calcareous nannoplankton evolution: a tale of climatic deterioration In: Prothero, D.R.,  
843 Berggren, W.A. (Eds.), *Eocene/Oligocene Climatic and Biotic Evolution*, Princeton University Press, Princeton, NJ,  
844 pp.272-309, 1992.
- 845 [Baatsen, M., Heydt, A. S. V. D., Huber, M., Kliphuis, M. A., Bijl, P. K., Sluijs, A., & Dijkstra, H. A. The middle to late  
846 Eocene greenhouse climate modelled using the CESM 1.0.5. \*Climate of the Past\*, 16, 2573-2597.  
847 <https://doi.org/10.5194/cp-16-2573-2020>, 2020.](https://doi.org/10.5194/cp-16-2573-2020)
- 848 Baldauf, J. G., & Barron, J. A. 29. Diatom Biostratigraphy: Kerguelen Plateau and Prydz Bay regions of the Southern  
849 Ocean. In: Barron, J., Larsen, B. et al. (1991) *Proceedings of the Ocean Drilling Program, Scientific Results*, v 119,  
850 1991
- 851 Barker, P.E, Kennett, J.P., et al. Proc. ODP, Init. Repts., 113: College Station, TX (Ocean Drilling Program).  
852 doi:10.2973/odp.proc.ir.113.1988.
- 853 Barker, P.F. Scotia Sea regional tectonic evolution: implications for mantle flow and palaeocirculation. *Earth-Science*  
854 *Reviews*, 55, 1-39 [https://doi.org/10.1016/S0012-8252\(01\)00055-1](https://doi.org/10.1016/S0012-8252(01)00055-1), 2001
- 855 [Barker, P. and Thomas, E. Origin, signature and palaeoclimatic influence of the Antarctic Circumpolar Current. \*Earth-\*  
856 \*Science Reviews\*, 66, 143-162, 2004.](https://doi.org/10.1016/S0012-8252(04)00055-1)
- 857 Barron, J., Larsen, B., et al. Proc. ODP, Init. Repts., 119: College Station, TX (Ocean Drilling Program).  
858 doi:10.2973/odp.proc.ir.119.1989.
- 859 Beerling, D., Royer, D. Convergent Cenozoic CO<sub>2</sub> history. *Nature Geoscience*, 4, 418-420  
860 <https://doi.org/10.1038/ngeo1186>, 2011.
- 861 Berggren, W.A., Kent, D.V., Swisher, C.C., III, and Aubry, M.P. A revised Cenozoic geochronology and  
862 chronostratigraphy, in Berggren, W.A., et al., eds., *Geochronology, time scales and global stratigraphic correlation:*



- 863 Framework for an historical geology: SEPM (Society for Sedimentary Geology) Special Publication 54, p. 129–212,  
864 1995.
- 865 Berner, R. A., Lasaga, A. C. & Garrels, R. M. The carbonate-silicate geochemical cycle and its effect on atmospheric  
866 carbon dioxide over the past 100 million years. *Am. J. Sci.* 283, 641–683, 1983.
- 867 [Bijl, P.K., Houben, A. J. P., Schouten, S., Bohaty, S. M., Sluijs, A., Reichart, G.-J., Sinninghe Damste, J.S., and](#)  
868 [Brinkhuis, H. Transient Middle Eocene atmospheric CO<sub>2</sub> and temperature variations. \*Science\*, 330, 819-821, 2010.](#)
- 869 [Billups, K., Channell, J.E.T. and Zachos, J. Late Oligocene to early Miocene geo- chronology and paleoceanography](#)  
870 [from the subantarctic South Atlantic. \*Paleoceanography\*, 17\(1\), 1004. doi:10.1029/2000PA000568, 2002.](#)
- 871 [Billups, K., Channell, J.E.T. and Zachos, J. Late Oligocene to early Miocene geo- chronology and paleoceanography](#)  
872 [from the subantarctic South Atlantic. \*Paleoceanography\*, 17\(1\), 1004. doi:10.1029/2000PA000568, 2002.](#)
- 873 [Bijl, P.K., Houben, A. J. P., Schouten, S., Bohaty, S. M., Sluijs, A., Reichart, G.-J., Sinninghe Damste, J.S., and](#)  
874 [Brinkhuis, H. Transient Middle Eocene atmospheric CO<sub>2</sub> and temperature variations. \*Science\*, 330, 819-821, 2010.](#)
- 875 Bohaty, S. M. and Zachos, J. C. Significant Southern Ocean warming event in the late middle Eocene, *Geology*, 31,  
876 1017–1020, <https://doi.org/10.1130/G19800.1>, 2003.
- 877 Bohaty, S. M., Zachos, J.C., and Delaney, M.L. Foraminiferal Mg/Ca evidence for Southern Ocean cooling across the  
878 Eocene-Oligocene transition, *Earth Planetary Science Letters*, 317–318, 251–261, 2012.
- 879 [Boot, D., Von Der Heydt, A.S., and Dijkstra, H.A. Effect of the Atlantic Meridional Overturning Circulation on](#)  
880 [Atmospheric pCO<sub>2</sub> variations. \*Earth System Dynamics\*, <https://doi.org/10.5194/esd-13-1041-2022>, 2022](#)
- 881 [Brandt, A., Bathmann, U., Brix, S., Cisewski, B., Flores, H., Göcke, C., et al. Maud Rise – A snapshot through the water](#)  
882 [column. \*Deep Sea Res. II\* 58, 1962–1982. doi: 10.1016/j.dsr2.2011.01.008, 2011.](#)
- 883 [Breecker, D. & Retallack, G. Refining the pedogenic carbonate atmospheric CO<sub>2</sub> proxy and application to Miocene](#)  
884 [CO<sub>2</sub>. \*Palaeogeography, Palaeoclimatology, Palaeoecology\*, 406, 1-8. <https://doi.org/10.1016/j.palaeo.2014.04.012>,](#)  
885 [2014.](#)
- 886 [Boot, D., Von Der Heydt, A.S., and Dijkstra, H.A. Effect of the Atlantic Meridional Overturning Circulation on](#)  
887 [Atmospheric pCO<sub>2</sub> variations. \*Earth System Dynamics\*, <https://doi.org/10.5194/esd-13-1041-2022>, 2022](#)
- 888 Carter, L., McCave, I.N., Williams, M.J.M. Chapter 4 Circulation and Water Masses of the Southern Ocean: A Review,  
889 Developments in Earth and Environmental Sciences, *Elsevier*, v. 8, 85-114, <https://doi.org/10.1016/S1571->  
890 [9197\(08\)00004-9](#), 2008.
- 891 Carter, A., Riley, T.R., Hillenbrand, C.D., Rittner, M. Widespread Antarctic glaciation during the Late Eocene, *Earth*  
892 [and Planetary Science Letters](#), 458, 49-57, <https://doi.org/10.1016/j.epsl.2016.10.045>, 2017.
- 893 Channell, J. E. T., Galeotti, S., Martin, E.E., Billups, K., Scher, H.D., and Stoner, J.S. Eocene to Miocene  
894 magnetostratigraphy, biostratigraphy and chemostratigraphy at ODP Site 1090 (sub-Antarctic South Atlantic), *Geol.*  
895 *Soc. Am. Bull.*, 115, 607–623, 2003.
- 896 Chapman, C.C., Lea, MA., Meyer, A. Defining Southern Ocean fronts and their influence on biological and physical  
897 processes in a changing climate. *Nature Climate Change*, 10, 209–219, <https://doi.org/10.1038/s41558-020-0705-4>,  
898 2020.
- 899 Clark, W. C. (ed.). Carbon Dioxide Review: 1982, p. 468, *Oxford University Press*, New York, 1982.
- 900 Cooke, P.J., Nelson, C.S., Crundwell, M.P., Spiegler, D. Bolboforma as monitors of Cenozoic palaeoceanographic  
901 changes in the Southern Ocean, *Palaeogeography, Palaeoclimatology, Palaeoecology*, Volume 188, Issues 1–2, 73-  
902 100, [https://doi.org/10.1016/S0031-0182\(02\)00531-X](https://doi.org/10.1016/S0031-0182(02)00531-X), 2002.
- 903 Coxall, H.K., Wilson, P.A., Pälike, H., Lear, C.H., Backman, J. Rapid stepwise onset of Antarctic glaciation and deeper  
904 calcite compensation in the Pacific Ocean. *Nature*, 433, 53–57. <https://doi.org/10.1038/nature03135>, 2005.
- 905 Coxall, H., Pearson, P.N. The Eocene-Oligocene transition, In: Williams, M., Haywood, A.M., Gregory, F.J., Schmidt,  
906 D.N. (Eds.), *Deep-Time Perspectives on Climate Change: Marrying the Signal from Computer Models and*  
907 *Biological Proxies*. pp. 351–387, 2007.
- 908 Coxall, H. K., & Wilson, P. A. Early Oligocene glaciation and productivity in the eastern equatorial Pacific: Insights  
909 into global carbon cycling, *Paleoceanography*, 26, PA2221, <https://doi.org/10.1029/2010PA002021>, 2011.
- 910 [Coxall, H.K., Huck, C.E., Huber, M. Export of nutrient rich Northern Component Water preceded early Oligocene](#)  
911 [Antarctic glaciation. \*Nature Geoscience\* 11, 190–196, 2018.](#)
- 912 [Cramer, B. S., J. R. Toggweiler, J. D. Wright, M. E. Katz, and K. G. Miller. Ocean overturning since the Late](#)  
913 [Cretaceous: Inferences from a new benthic foraminiferal isotope compilation. \*Paleoceanography\*, 24, PA4216;](#)  
914 [doi:10.1029/2008PA001683, 2009.](#)
- 915 Dalai, T.K. et al. The Late Eocene 1870s/1880s excursion: Chemostratigraphy, cosmic dust flux and the Early  
916 Oligocene glaciation. *Earth and Planetary Science Letters*, 241(3-4), 477-492,  
917 <https://doi.org/10.1016/j.epsl.2005.11.035>, 2006.
- 918 De Baar, H., de Jong, J., Bakker, D. et al. Importance of iron for plankton blooms and carbon dioxide drawdown in the  
919 Southern Ocean. *Nature*, 373, 412–415 <https://doi.org/10.1038/373412a0>, 1995.
- 920 DeConto, R. & Pollard, D. Rapid Cenozoic glaciation of Antarctica induced by declining atmospheric CO<sub>2</sub>. *Nature*, 421,  
921 245–249. <https://doi.org/10.1038/nature01290>, 2003.

- 922 [DeConto RM, Pollard D, Wilson PA, Palike H, Lear CH, Pagani M. Thresholds for Cenozoic bipolar glaciation.](#)  
923 [doi:10.1038/nature07337, 2008.](#)
- 924 [Deppeler, S.L. and Davidson, A.T. Southern Ocean Phytoplankton in a Changing Climate. \*Frontiers in Marine Science.\*](#)  
925 [4, <https://www.frontiersin.org/articles/10.3389/fmars.2017.00040>, 2017.](#)
- 926 [DeVries, T. The Ocean Carbon Cycle. \*Annual Review of Environment and Resources\*, 47, pp. 317-341.](#)  
927 [http://dx.doi.org/10.1146/annurev-environ-120920-111307, 2022.](#)
- 928 [DeConto RM, Pollard D, Wilson PA, Palike H, Lear CH, Pagani M. Thresholds for Cenozoic bipolar glaciation-](#)  
929 [doi:10.1038/nature07337, 2008-](#)
- 930 [Diekmann, B., Kuhn, G., Gersonde, R., Mackensen, A. Middle Eocene to early Miocene environmental changes in the](#)  
931 [sub-Antarctic Southern Ocean: evidence from biogenic and terrigenous depositional patterns at ODP Site 1090, \*Global\*](#)  
932 [and Planetary Change, Volume 40, Issues 3–4, Pages 295–313, <https://doi.org/10.1016/j.gloplacha.2003.09.001>, 2004.](#)
- 933 Diester-Haass, L. Late Eocene-Oligocene sedimentation in the Antarctic Ocean, Atlantic Sector (Maud Rise, ODP leg  
934 113, Site 689), Development of surface and bottom water circulation, in *The Antarctic Paleoenvironment: A*  
935 *Perspective on Global Change, Part 1, Antarct. Res. Ser.*, vol. 56, edited by J. P. Kennett, and D. A. Warnke, pp. 185–  
936 202, AGU, Washington, D. C, 1992.
- 937 Diester-Haass, L. Middle Eocene to early Oligocene Paleooceanography of the Antarctic Ocean (Maud Rise, ODP Leg  
938 113, Site 689): change from a low to a high productivity ocean. *Paleogeography, Paleoclimatology, Paleoecology*,  
939 113, 311-334. [https://doi.org/10.1016/0031-0182\(95\)00067-V](https://doi.org/10.1016/0031-0182(95)00067-V), 1995.
- 940 Diester-Haass, L. Late Eocene-Oligocene paleoceanography in the southern Indian Ocean (ODP Site 744). *Marine*  
941 *Geology*, 130, 99-119, 1996.
- 942 Diester-Haass, L & Zahn, R. Eocene-Oligocene transition in the Southern Ocean: History of water mass circulation and  
943 biological productivity, *Geology*, 24, 163–166. 1996.
- 944 Diester-Haass, L & Zahn, R. Paleoproductivity increase at the Eocene-Oligocene climatic transition: ODP/DSDP Sites  
945 763 and 592. *Paleogeography, Paleoclimatology, Paleoecology*, 172, 153-170. [https://doi.org/10.1016/S0031-](https://doi.org/10.1016/S0031-0182(01)00280-2)  
946 [0182\(01\)00280-2](#), 2001.
- 947 Diester-Haass, L. & Zachos, J. The Eocene-Oligocene transition in the Equatorial Atlantic (ODP Site 925);  
948 paleoproductivity increase and positive  $\delta^{13}C$  excursion. In Prothero, D.R; Ivany, L. C; Nesbitt, E. A. (eds) *From*  
949 *greenhouse to icehouse; the marine Eocene-Oligocene transition*, *Columbia University Press*, New York, NY, United  
950 States (USA), 2003.
- 951 Diester-Haass, L., & Faul, K. Paleoproductivity reconstructions for the Paleogene Southern Ocean: A direct comparison  
952 of geochemical and micropaleontological proxies. *Paleoceanography and Paleoclimatology*, 34(1), 79– 97.  
953 <https://doi.org/10.1029/2018PA003384>, 2019.
- 954 [Doria, G., Royer, D. L., Wolfe, A. P., Fox, A., Westgate, J. A., & Beerling, D. J. Declining atmospheric CO<sub>2</sub> during the](#)  
955 [late Middle Eocene climate transition. \*American Journal of Science\*, 311\(1\), 63-75.](#)  
956 [https://doi.org/10.2475/01.2011.03, 2011.](#)
- 957 Douglas, P.M.J., Affek, H.P., Ivany, L.C., Houben, A.J.P., Sijp, W.P., Sluijs, A., Schouten, S., Pagani, M. Pronounced  
958 zonal heterogeneity in Eocene southern high-latitude sea surface temperatures. *PNAS*, 111 (18) 6582-6587  
959 <https://doi.org/10.1073/pnas.1321441111>, 2014.
- 960 Dutkiewicz, A., Müller, R.D. The carbonate compensation depth in the South Atlantic Ocean since the Late Cretaceous.  
961 *Geology*, 49 (7): 873–878. <https://doi.org/10.1130/G48404.1>, 2021.
- 962 Dymond, J., Suess, E. and Lyle, M. Barium in Deep-Sea Sediment: A Geochemical Proxy for Paleoproductivity.  
963 *Paleoceanography and Paleoclimatology*, 7(2), 163-181. <https://doi.org/10.1029/92PA00181>, 1992.
- 964 [Egan, K.E., Rickaby, R.E.M., Hendry, K.R., Halliday, A.N. Opening the gateways for diatoms primes Earth for](#)  
965 [Antarctic glaciation. \*Earth Planetary Science Letters\* 375, 34–43. <https://doi.org/10.1016/j.epsl.2013.04.030>,](#)  
966 [2013](#)
- 967 [Ekart, D. D. A 400 million year carbon isotope record of pedogenic carbonate; implications for paleoatmospheric](#)  
968 [carbon dioxide. \*American Journal of Science\*, 299\(10\), 805-827. <https://doi.org/10.2475/ajs.299.10.805>, 1999.](#)
- 969 Elsworth, G., Galbraith, E., Halverson, G. et al. Enhanced weathering and CO<sub>2</sub> drawdown caused by latest Eocene  
970 strengthening of the Atlantic meridional overturning circulation. *Nature Geoscience*, 10, 213–216).  
971 <https://doi.org/10.1038/ngeo2888>, 2017.
- 972 [Erdei, B., Utescher, T., Hably, L., Roth-Nebelsick, A., & Grein, M. Early Oligocene Continental Climate of the](#)  
973 [Palaeogene Basin \(Hungary and Slovenia\) and the Surrounding Area. \*Turkish Journal of Earth Sciences\*, 21, 153-](#)  
974 [186. <https://doi.org/10.3906/yer-1005-29>, 2012.](#)
- 975 Faul K. L., Delaney, M. L. A comparison of early Paleogene export productivity and organic carbon burial flux for  
976 Maud Rise, Weddell Sea, and Kerguelen Plateau, south Indian Ocean. *Paleoceanography*, v.25, 3214, 2010.
- 977 [Falkowski P., Scholes R.J., Boyle E., Canadell J., Canfield D., Elser J., Gruber N., Hibbard K., Höglberg P., Linder S.,](#)  
978 [Mackenzie F.T., Moore III B., Pedersen T., Rosenthal Y., Seitzinger S., Smetacek V., Steffen W. The global carbon](#)  
979 [cycle: a test of our knowledge of earth as a system. \*Science\*, 290, 291–296. doi: 10.1126/science.290.5490.291-](#)  
980 [PMID: 11030643, 2000.](#)

- 981 Florindo, F. and Roberts, A. P. Eocene-Oligocene magnetobiochronology of ODP Sites 689 and 690, Maud Rise,  
982 Weddell Sea, Antarctica. *Geological Society of America Bulletin*, 117(1), 46–. doi:10.1130/b25541.1, 2005
- 983 Foster, G.; Royer, D. and Lunt, D. Future climate forcing potentially without precedent in the last 420 million years.  
984 *Nature Communications*, 8, 14845. <https://doi.org/10.1038/ncomms14845>, 2017.
- 985 Frank, M. Radiogenic isotopes: tracers of past ocean circulation and erosional input. *Rev. Geophys.* 40, 1001.  
986 doi:10.1029/2000RG000094, 2002.
- 987 Galeotti, S., Coccioni, R., Gersonde, R. Middle Eocene–Early Pliocene Subantarctic planktic foraminiferal  
988 biostratigraphy of Site 1090, Agulhas Ridge, Marine Micropaleontology, 45, 3–4, 357–381,  
989 [https://doi.org/10.1016/S0377-8398\(02\)00035-X](https://doi.org/10.1016/S0377-8398(02)00035-X), 2002. Gasson, E., Lunt, D. J., Deconto, R., Goldner, A.,  
990 Heinemann, M., Huber, M., Legrande, A. N., Pollard, D., Sagoo, N., Siddall, M., Winguth, A., and Valdes, P. J.:  
991 Uncertainties in the modelled CO<sub>2</sub> threshold for Antarctic glaciation. *Climate of the Past*, 10, 451–466,  
992 2014 Gersonde, R., Hodell, B.A., Blum, P., and Shipboard Scientific Party. Leg 177 summary, Proc. Ocean Drill.  
993 Program, Initial Rep., 177, 1–67, 1999.
- 994 Gersonde, R., Hodell, B.A., Blum, P., and Shipboard Scientific Party. Leg 177 summary, Proc. Ocean Drill. Program,  
995 Initial Rep., 177, 1–67, 1999.
- 996 Glass, B.P., Hall, C.M., and York, D. 40Ar/39Ar laser probe dating of North American tektite fragments from Barbados  
997 and the age of the Eocene-Oligocene boundary: *Chemical Geology*, v. 59, p. 181–186., 1996.
- 998 Goldner, A., Herold, N. and Huber, M. Antarctic glaciation caused ocean circulation changes at the Eocene-Oligocene  
999 transition, *Nature*, 511(7511), 574–577, doi:10.1038/nature13597, 2014.
- 1000 Gradstein, F. M., Ogg, J. G., Schmitz, M., & Ogg, G. The Geological Time Scale 2012 (pp. 1176). Oxford, UK:  
1001 Elsevier, 2012.
- 1002 Griffith, E. M., Thomas, E., Lewis, A. R., Penman, D. E., Westerhold, T., and Winguth, A. M.: Benthic-Pelagic  
1003 Decoupling: The Marine Biological Carbon Pump During Eocene Hyperthermals. *Paleoceanography and*  
1004 *Paleoclimatology*, 36, <https://doi.org/10.1029/2020PA004053>, 2021.
- 1005 Grein, M., Oehm, C., Konrad, W., Utescher, T., Kunzmann, L., and Roth-Nebelsick, A.: Atmospheric CO<sub>2</sub> from the late  
1006 Oligocene to early Miocene based on photosynthesis data and fossil leaf characteristics. *Palaeogeography,*  
1007 *Palaeoclimatology, Palaeoecology*, 374, 41–51, <https://doi.org/10.1016/j.palaeo.2012.12.025>, 2013.
- 1008 Henderiks, J., & Pagani, M. Coccolithophore cell size and the Paleogene decline in atmospheric CO<sub>2</sub>. *Earth and*  
1009 *Planetary Science Letters*, 269(3), 576–584. <https://doi.org/10.1016/j.epsl.2008.03.016>, 2008.
- 1010 Gruber, N., Landshützer, P., Lovenduski, N.S. The Variable Southern Ocean Carbon Sink. *Annual Review of Marine*  
1011 *Science*, 11, 159–186. <https://doi.org/10.1146/annurev-marine-121916-063407>, 2019.
- 1012 Hayes, C.T.; Costa, K.M.; Anderson, R.F.; Calvo, E.; Chase, Z.; Demina, L.L.; Dutay, J.; German, C.R.; Heimbürger-  
1013 Boavida, L.; Jaecard, S.L.; et al. Global Ocean Sediment Composition and Burial Flux in the Deep Sea. *Global*  
1014 *Biogeochem. Cycles* 35, 2021.
- 1015 Henehan, M.; Edgar, K.M.; Foster, G.L., Penman, D.E.; Hull, P.M.; Greenop, R.; Anagnostou, E.; Pearson, P.N.  
1016 Revisiting the Middle Eocene Climatic Optimum “Carbon Cycle Conundrum” with New Estimates of Atmospheric  
1017 pCO<sub>2</sub> from Boron Isotopes. *Paleoceanography and Paleoclimatology*. 35(6). <https://doi.org/10.1029/2019PA003713>,  
1018 2020.
- 1019 Hill, D. J., Haywood, A. M., Valdes, P. J., Francis, J. E., Lunt, D. J., Wade, B. S., and Bowman, V. C.: Paleogeographic  
1020 controls on the onset of the Antarctic circumpolar current, *Geophysical Research Letters*, 40, 5199–5204, 2013.
- 1021 Houben, A.J.P., van Mourik, C.A., Montanari, A., Coccioni, R., Brinkhuis, H. The Eocene–Oligocene transition:  
1022 Changes in sea level, temperature or both? *Palaeogeography, Palaeoclimatology, Palaeoecology*. 335–336, p 75–83  
1023 <https://doi.org/10.1016/j.palaeo.2011.04.008>, 2012.
- 1024 Houben, A. J. P., Bijl, P. K., Sluijs, A., Schouten, S., and Brinkhuis, H.: Late Eocene Southern Ocean cooling and  
1025 invigoration of circulation preconditioned Antarctica for full scale glaciation, *Geochemistry, Geophysics,*  
1026 *Geosystems*, 20, <https://doi.org/10.1029/2019GC008182>, 2019.
- 1027 Huber, B.T. and Quillevère, F. Revised Paleogene Planktonic Foraminiferal biozonation for the Austral realm. *Journal*  
1028 *of Foraminiferal Research*, 35(4), 299–314., 2005.
- 1029 Huber, M., Brinkhuis, H., Stickley, C.E., Döös, K., Sluijs, A., Warner, J., Schellenberg, S.A. and Williams, G.L. Eocene  
1030 circulation of the Southern Ocean: Was Antarctica kept warm by subtropical waters? *Paleoceanography*, 19,  
1031 doi:10.1029/2004PA001014, 2004.
- 1032 Huber, M. and Nof, D. The ocean circulation in the southern hemisphere and its climatic impacts in the Eocene.  
1033 *Palaeogeography, Palaeoclimatology, Palaeoecology*, 231, 9–28, <https://doi.org/10.1016/j.palaeo.2005.07.037>  
1034 2006.
- 1035 Huber, M. and Nof, D. The ocean circulation in the southern hemisphere and its climatic impacts in the Eocene.  
1036 *Palaeogeography, Palaeoclimatology, Palaeoecology* 231, 9–28, 2006.
- 1037 Huck, C. E., van de Flierdt, T., Bohaty, S. M. and Hammond, S. J. Antarctic climate, Southern Ocean circulation  
1038 patterns, and deep-water formation during the Eocene. *Paleoceanography*, 32, 674– 691.  
1039 <https://doi.org/10.1002/2017PA003135>, 2017.



- 1040 Hutchinson, D.K., Coxall, H.K., Lunt, D.J., Steinthorsdottir, M., de Boer, A.M. et al. The Eocene-Oligocene transition:  
1041 A review of marine and terrestrial proxy data, models and model-data comparisons. *Climate of the Past*, 17(1), 269-  
1042 315, 2021.
- 1043 Inglis, G. N., Farnsworth, A., Lunt, D., Foster, G. L., Hollis, C. J., Pagani, M., Jardine, P. E., Pearson, P. N., Markwick,  
1044 P., Galsworthy, A. M. J., Raynham, L., Taylor, K. W. R. and Pancost, R. D. Descent toward the Icehouse: Eocene sea  
1045 surface cooling inferred from GDGT distributions, *Paleoceanography*, 30(7), 1000–1020,  
1046 doi:10.1002/2014PA002723, 2015.
- 1047 Inokuchi, H; Heider, F. Paleolatitude of the southern Kerguelen Plateau inferred from the paleomagnetic study of late  
1048 Cretaceous basalts. In: Wise, SW; Schlich, R; et al. (eds.), Proceedings of the Ocean Drilling Program, Scientific  
1049 Results, College Station, TX (Ocean Drilling Program), 120, 89-96,  
1050 <https://doi.org/10.2973/odp.proc.sr.120.129.1992>
- 1051 IPCC. Climate Change 2021: The Physical Science Basis. Working Group I Contribution to the Sixth Assessment  
1052 Report of the Intergovernmental Panel on Climate Change. *Cambridge University Press*, Cambridge, United  
1053 Kingdom and New York, NY, USA, 2391pp, 2021.
- 1054 [Katz, M.E., Cramer, B.S., Toggweiler, J.R., Esmay, G., Liu, C., Miller, K.G., Rosenthal, Y., Wade, B.S., Wright J.D.](#)  
1055 [Impact of Antarctic Circumpolar Current Development on Late Paleogene Ocean Structure. \*Science\*, 332, 1076-](#)  
1056 [1079, DOI: 10.1126/science.1202122, 2011.](#)
- 1057 [Kennet, J.P. Cenozoic evolution of Antarctic glaciation, the circum-Antarctic Ocean, and their impact on global](#)  
1058 [paleoceanography. \*Journal of Geophysical Research\*, 82, 3843-3860,](#)  
1059 [https://doi.org/10.1029/JC082i027p03843.1977.](https://doi.org/10.1029/JC082i027p03843.1977)
- 1060 [Katz, M.E., Cramer, B.S., Toggweiler, J.R., Esmay, G., Liu, C., Miller, K.G., Rosenthal, Y., Wade, B.S., Wright J.D.](#)  
1061 [Impact of Antaretic Circumpolar Current Development on Late Paleogene Ocean Structure. \*Science\*, 332, 1076-](#)  
1062 [1079, 2011.](#)
- 1063 [Kennet, J.P. Cenozoic evolution of Antaretic glaciation, the circum-Antaretic Ocean, and their impact on global](#)  
1064 [paleoceanography. \*J. Geophys. Res.\*, 82, 3843-3860, 1977.](#)
- 1065 Kennett, J.P. and Stott, L.D. Proteus and Proto- Oceanus: ancestral Paleogene oceans as revealed from antarctic stable  
1066 isotopic results: ODP Leg 113. In: Leg 113. ODP Sci. Res., pp. 865-880, 1990.
- 1067 Kim J.H., Crosta, X., Michel, E., Schouten, S., Duprat, J., Damsté, J.S.S. Impact of lateral transport on organic proxies  
1068 in the Southern Ocean, *Quaternary Research*, 71(2), 246-250. <https://doi.org/10.1016/j.yqres.2008.10.005>, 2009.
- 1069 Kim, Yong Sun, Orsi, Alejandro H. On the Variability of Antarctic Circumpolar Current Fronts Inferred from 1992–  
1070 2011 Altimetry. *Journal of Physical Oceanography*, 3054–3071. <https://doi.org/10.1175/JPO-D-13-0217.1>, 2014.
- 1071 [Kohn, M. J., Strömberg, C. A., Madden, R. H., Dunn, R. E., Evans, S., Palacios, A., & Carlini, A. A. Quasi-static](#)  
1072 [Eocene–Oligocene climate in Patagonia promotes slow faunal evolution and mid-Cenozoic global cooling.](#)  
1073 [\*Palaeogeography, Palaeoclimatology, Palaeoecology\*, 435, 24-37. <https://doi.org/10.1016/j.palaeo.2015.05.028>,](#)  
1074 [2015.](#)
- 1075 Kuhlbrodt, T., Griesel, A., Montoya, M., Levermann, A., Hofmann, M., Rahmstorf, S. On the driving processes of the  
1076 Atlantic meridional overturning circulation. *Reviews of Geophysics*, 45, RG2001, doi:10.1029/2004RG000166,  
1077 2007.
- 1078 [Kürschner, W. M., Kvaček, Z., & Dilcher, D. L. The impact of Miocene atmospheric carbon dioxide fluctuations on](#)  
1079 [climate and the evolution of terrestrial ecosystems. \*Proceedings of the National Academy of Sciences\*, 105\(2\), 449-](#)  
1080 [453 <https://doi.org/10.1073/pnas.0708588105>, 2008.](#)
- 1081 Ladant, J.-B., Donnadieu, Y. and Dumas, C. Links between CO<sub>2</sub>, glaciation and water flow: reconciling the Cenozoic  
1082 history 1680 of the Antarctic Circumpolar Current, *Climate of the Past*, 10(6), 1957–1966, doi:10.5194/cp-10-1957-  
1083 2014, 2014.
- 1084 Lauretano, V., Kennedy-Asser, A.T., Korasidis, V.A., Wallace, M.W., Valdes, P.J., Lunt, D.J., Pancost, R.D. and Naafs,  
1085 B.D.A. Eocene to Oligocene terrestrial Southern Hemisphere cooling caused by declining pCO<sub>2</sub>. *Nature Geoscience*  
1086 14, 659–664. <https://doi.org/10.1038/s41561-021-00788-z>, 2021.
- 1087 Lazarus, D. and Caulet J.P. Cenozoic Southern Ocean reconstructions from sedimentologic, radiolarian, and other  
1088 microfossil data. In: J.P. Kennett and D.A. Warnke, Eds., The Antarctic Paleoenvironment: A perspective on global  
1089 change. Pt. 2. *Antarctic Research Series*, 60: 145-174, 1994.
- 1090 Li, Z., Lozier, M.S., Cassar, N. Linking Southern Ocean Mixed Layer Dynamics to Net Community Production on  
1091 Various Timescales. *JGR Oceans*, 126. <https://doi.org/10.1029/2021JC017537>, 2021.
- 1092 Liu, Z., M., Pagani, D., Zinniker, R., DeConto, M., Huber, H., Brinkhuis, S. R., Shah, R. M. Leckie, and Pearson, A.  
1093 Global cooling during the Eocene – Oligocene climate transition, *Science*, 323, 1187–1190, 2009.
- 1094 Livermore, R., Nankivell, Eagles, G. and Morris, P. Paleogene opening of Drake Passage, *Earth Planetary Science*  
1095 [Letters](#), 236, 459–470, 2005.
- 1096 Livermore, R., Hillenbrand, C., Meredith, M., and Eagles, G. Drake Passage and Cenozoic climate: an open and shut  
1097 case?, *Geochemistry: Geophysics: Geosystems*, 8, Q01005, <https://doi.org/10.1029/2005GC001224>, 2007.

- 1098 [Mackensen, A., and Ehrmann, W.U. Middle Eocene through Early Oligocene climate history and paleoceanography in](#)  
1099 [the Southern Ocean: Stable oxygen and carbon isotopes from ODP Sites on Maud Rise and Kerguelen Plateau,](#)  
1100 [Marine Geology, 108, 1–27, https://doi.org/10.1016/0025-3227\(92\)90210-9, 1992.](#)
- 1101 ~~Mackensen, A., and Ehrmann, W.U. Middle Eocene through Early Oligocene climate history and paleoceanography in~~  
1102 ~~the Southern Ocean: Stable oxygen and carbon isotopes from ODP Sites on Maud Rise and Kerguelen Plateau, Mar-~~  
1103 ~~Geol., 108, 1–27, 1992.~~
- 1104 Marino, M. and Flores, J.A. Middle Eocene to early Oligocene calcareous nannofossil stratigraphy at Leg 177 Site  
1105 1090, *Marine Micropaleontology*, 45, 383–398, 2002.
- 1106 Martin, E.E. and Haley, B.A. Fossil fish teeth as proxies for seawater Sr and Nd isotopes. *Geochimica et Cosmochimica*  
1107 *Acta*, 64 (5), 835–847, doi:10.1016/S0016-7037(99)00376-2, 2000.
- 1108 Martin, E.E. and Scher, H.D. Preservation of seawater Sr and Nd isotopes in fossil fish teeth: bad news and good news.  
1109 *Earth and Planetary Science Letters*, 220(1-2), 25–39, https://doi.org/10.1016/S0012-821X(04)00030-5, 2004.
- 1110 ~~Mazloff, M.R., Heimbach, P., Wunsch, C. An eddy-permitting Southern Ocean state estimate. J. Phys. Oceanogr. 40,~~  
1111 ~~880–899, 2010.~~
- 1112 Mikolajewicz, U., Maier-Reimer, E., Crowley, T. J. and Kim, K.-Y. Effect of Drake and Panamanian Gateways on the  
1113 circulation of an ocean model, *Paleoceanography*, 8(4), 409–426, doi:10.1029/93PA00893, 1993.
- 1114 Miller, K.G. Janecek, T.R., Katz, M.E., Keil, D.J. Abyssal circulation and benthic foraminiferal changes near the  
1115 Paleocene/Eocene boundary. *Paleoceanography*, 2(6), 741–761, https://doi.org/10.1029/PA002i006p00741, 1987.
- 1116 ~~Miller, K.G., Wright, J.D., Katz, M.E., Wade, B., Browning, J.V., Cramer, B.S., and Rosenthal, Y. Climate threshold at~~  
1117 ~~the Eocene-Oligocene transition: Antarctic ice sheet influence on ocean circulation, in Koeberl, C., and Montanari,~~  
1118 ~~A., ed., The Late Eocene Earth Hot house, Icehouse, and Impacts: Geological Society of America Special Paper 452,~~  
1119 ~~p. 169–178, doi:10.1130/2009.2452 (11), 2009.~~
- 1120 Moore, J. K., M. R. Abbott, J. G. Richman, W. O. Smith, T. J. Cowles, K. H. Coale, W. D. Gardner, and R. T. Barber.  
1121 SeaWiFS satellite ocean color data from the Southern Ocean, *Geophysical Research Letters*, 26, 1465–1468, 1999.
- 1122 Muza, J.P., Williams, D.F., Wise, S.W. Paleogene oxygen record for Deep Sea Drilling Project Sites 511 and 512,  
1123 subantarctic South Atlantic Ocean: Paleotemperatures, paleoceanographic changes, and the Eocene/Oligocene  
1124 boundary event. In: Ludwig, WJ; Krasheninnikov, VA; et al. (Eds.), Initial Reports of the Deep-Sea Drilling Project  
1125 (U.S. Govt. Printing Office), 71, 409–422, https://doi.org/10.2973/dsdp.proc.71.117.1983, 1983.
- 1126 Najjar, R.G., Nong, G.T., Seidov, D., Peterson, W.H. Modelling geographic impacts on early Eocene ocean temperature,  
1127 *Geophysical Research Letters*, 29 (15), 401–404. https://doi.org/10.1029/2001GL014438, 2002.
- 1128 Nelson, D.M. & Smith, W. Sverdrup revisited: Critical depths, maximum chlorophyll levels, and the control of Southern  
1129 Ocean productivity by the irradiance-mixing regime. *Limnology and Oceanography*. 36, 1650–1661.  
1130 https://doi.org/10.4319/lo.1991.36.8.1650, 1991.
- 1131 Nielsen, E.B., Anderson, L.D., Delaney, M.L. Paleoproductivity, nutrient burial, climate change and the carbon cycle in  
1132 the western equatorial Atlantic across the Eocene/Oligocene boundary. *Paleoceanography*, v 18, n. 3, 1057,  
1133 doi:10.1029/2002PA000804, 2003.
- 1134 [Nooteboom, P. D., Baatsen, M., Bijl, P. K., Kliphuis, M. A., van Sebille, E., Sluijs, A., Dijkstra, H. A., and von der](#)  
1135 [Heydt, A. S.: Improved Model-Data Agreement With Strongly Eddying Ocean Simulations in the Middle-Late](#)  
1136 [Eocene. \*Paleoceanography and Paleoclimatology\*. 37, 10.1029/2021PA004405, 2022.](#)
- 1137 O'Brien, C. L., Huber, M., Thomas, E., Pagani, M., Super, J. R., Elder, L. E., Hull, P. M. The enigma of Oligocene  
1138 climate and global surface temperature evolution. *Proceedings of the National Academy of Sciences* Oct 2020, 117  
1139 (41) 25302–25309; doi:10.1073/pnas.2003914117, 2020.
- 1140 [Olivarez Lyle, A., and M. W. Lyle. Missing organic carbon in Eocene marine sediments: Is metabolism the biological](#)  
1141 [feedback that maintains end-member climates?, \*Paleoceanography\*. 21, PA2007, doi:10.1029/2005PA001230, 2006.](#)
- 1142 Orsi, A.H., Whitworth, T., Nowlin, W.D. On the meridional extent and fronts of the Antarctic Circumpolar Current,  
1143 Deep Sea Research Part I: *Oceanographic Research Papers*, v 42, 5, 641–673, https://doi.org/10.1016/0967-  
1144 0637(95)00021-W, 1995.
- 1145 [Pagani, M. Late Miocene Atmospheric CO<sub>2</sub> Concentrations and the Expansion of C4 Grasses. \*Science\*, 285\(5429\), 876-](#)  
1146 [879. https://doi.org/10.1126/science.285.5429.876, 1999.](#)
- 1147 [Pagani, M., Arthur, M. A., & Freeman, K. H. Miocene evolution of atmospheric carbon dioxide. \*Paleoceanography\*,](#)  
1148 [14\(3\), 273–292. https://doi.org/10.1029/1999pa900006, 1999.](#)
- 1149 Pagani, M., Zachos, J. C., Freeman, K. H., Tipler, B., and Bohaty, S. Marked decline in atmospheric carbon dioxide  
1150 concentrations during the Paleogene. *Science*, 309 600–603. DOI: 10.1126/science.111006, 2005
- 1151 Pagani, M., Huber, M., Liu, Z., Bohaty, S.M., Henderiks, J., Sijp, W., Krishnan, S. & DeConto, R.M. The role of carbon  
1152 dioxide during the onset of Antarctic glaciation. *Science*, 334, 1261–1264. DOI: 10.1126/science.1203909, 2011.
- 1153 Pälike, H., Lyle, M.W., Nishi, H., Raffi, I., Ridgwell, A., Gamage, K., Klaus, A., Acton, G., Anderson, L., Backman, J.,  
1154 Baldauf, J., Beltran, C., Bohaty, S.M., Bown, P., Busch, W., Channell, J.E.T., Chun, C.O.J., Delaney, M., Dewangan,  
1155 P., Dunkley Jones, T., Edgar, K.M., Evans, H., Fitch, P., Foster, G.L., Gussone, N., Hasegawa, H., Hathorne, E.C.,  
1156 Hayashi, H., Herrle, J.O., Holbourn, A., Hovan, S., Hyeong, K., Iijima, K., Ito, T., Kamikuri, S., Kimoto, K.,



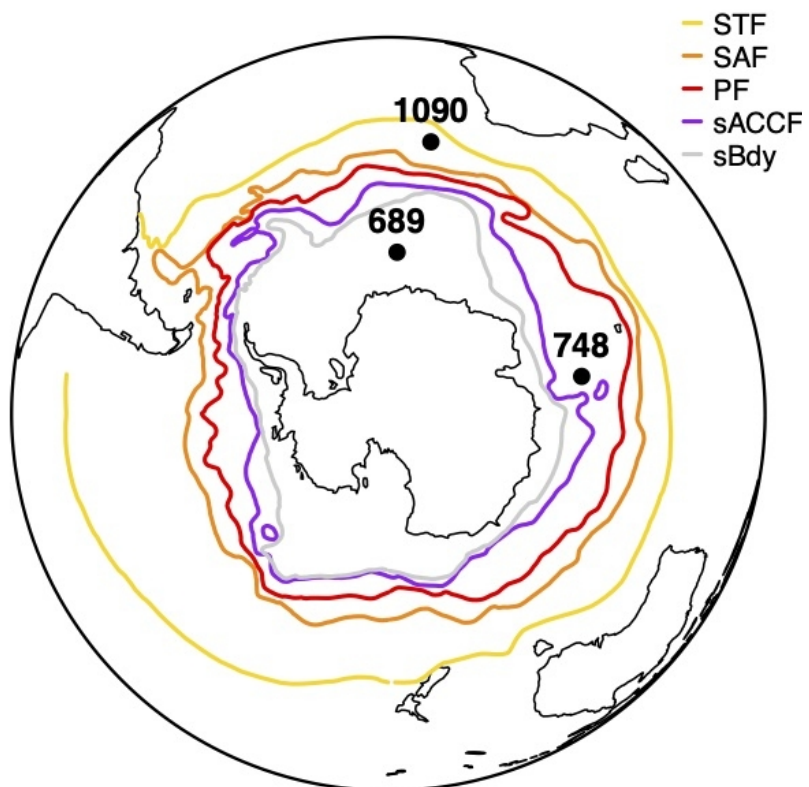
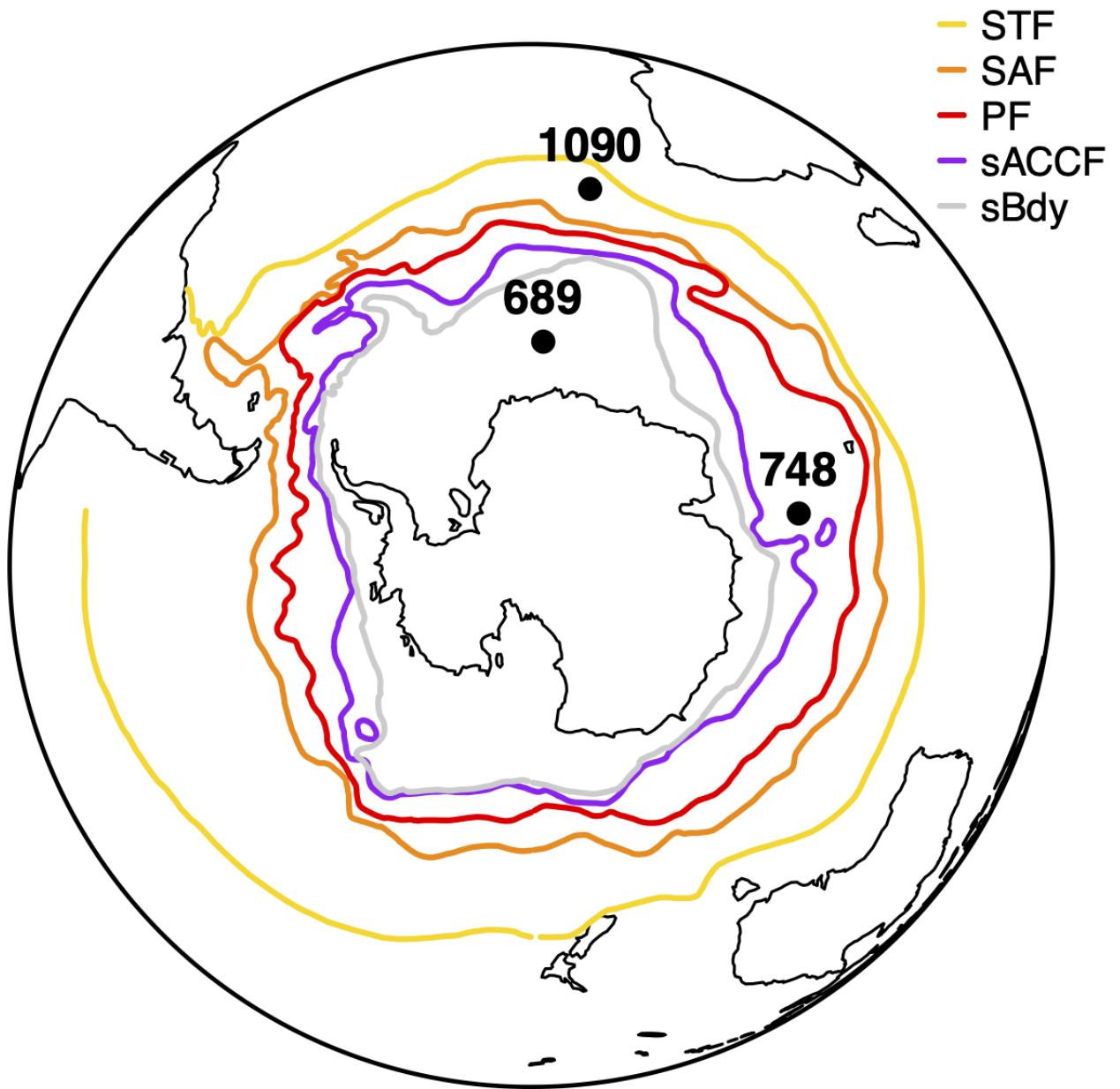
- 1157 Kuroda, J., Leon-Rodriguez, L., Malinverno, A., Moore, T.C., Murphy, B.H., Murphy, D.P., Nakamura, H., Ogane,  
 1158 K., Ohneiser, C., Richter, C., Robinson, R., Rohling, E.J., Romero, O., Sawada, K., Scher, H., Schneider, L., Sluijs,  
 1159 A., Takata, H., Tian, J., Tsujimoto, A., Wade, B.S., Westerhold, T., Wilkens, R., Williams, T., Wilson, P.A.,  
 1160 Yamamoto, Y., Yamamoto, S., Yamazaki, T., Zeebe, R.E. A Cenozoic record of the equatorial Pacific carbonate  
 1161 compensation depth, *Nature*, 488 (7413), 609-615, doi:10.1038/nature11360, 2012.
- 1162 Palter, J. B., Sarmiento, J. L., Marinov, I. & Gruber, N. In: *Chemical Oceanography of Frontal Zones* (ed. Belkin, I. M.)  
 1163 [https://doi.org/10.1007/698\\_2013\\_241](https://doi.org/10.1007/698_2013_241) (Springer), 2013.
- 1164 ~~Park Y. H., Park T., Kim T.W., Lee S.H., Hong C.S., Lee J.H., Rio M.H., Pujol M.I., Ballarotta M., Durand I., Provost  
 1165 C. Observations of the Antarctic Circumpolar Current over the Udintsev Fracture Zone, the narrowest choke point in the  
 1166 Southern Ocean. *Journal of Geophysical Research: Oceans*, -. <https://doi.org/10.1029/2019JC015024>, 2019.~~
- 1167 ~~Pearson, P. & Palmer, M.R. Atmospheric carbon dioxide concentrations over the past 60 million years. *Nature*, 206,  
 1168 695-699, 2000.~~
- 1169 Pearson, P., Foster, G. and Wade, B. Atmospheric carbon dioxide through the Eocene–Oligocene climate transition.  
 1170 *Nature*, 461, 1110–1113. <https://doi.org/10.1038/nature08447>, 2009.
- 1171 Persico, D., and Villa, G. High-resolution calcareous nannofossil biostratigraphy and palaeoecology from Eocene-  
 1172 Oligocene sediments, Maud Rise, Weddell Sea, and Kerguelen Plateau, Antarctica: University of Parma, Italy,  
 1173 Abstract 9th International Nannoplankton Association Conference, 8th–14th September 2002.
- 1174 Persico, D., and Villa, G. Eocene-Oligocene calcareous nannofossils from Maud Rise and Kerguelen Plateau  
 1175 (Antarctica): Palaeoecological and palaeoceanographic implications: *Marine Micropaleontology*, v. 52, p. 153–179,  
 1176 doi: 10.1016/j.marmicro.2004.05.002, 2004.
- 1177 ~~Pfuhl, H. A. & McCave, I. N. Evidence for late Oligocene establishment of the Antarctic Circumpolar Current. *Earth  
 1178 and Planetary Science Letters*, 235, 715–728, 2005.~~
- 1179 ~~Pieprgras D.J., Wasserburg G.J. Isotopic composition of neodymium in waters from the drake passage. *Science Jul  
 1180 16;217(4556):207-14. doi: 10.1126/science.217.4556.207, 1982.*~~
- 1181 ~~Pieprgras D.J., Wasserburg G.J. Isotopic composition of neodymium in waters from the drake passage. *Science Jul  
 1182 16;217(4556):207-14. doi:10.1126/science.217.4556.207, 1992.*~~
- 1183 ~~Pfuhl, H. A. & McCave, I. N. Evidence for late Oligocene establishment of the Antarctic Circumpolar Current. *Earth  
 1184 and Planetary Science Letters*, 235, 715–728, 2005.~~
- 1185 Prothero, D.R. & Berggren, W.A. Eocene-Oligocene Climatic and Biotic Evolution. *Princeton University Press*,  
 1186 Princeton, NJ, 1992.
- 1187 Pusz, A. E., Thunell, R.C. and Miller, K.G. Deep water temperature, carbonate ion, and ice volume changes across the  
 1188 Eocene-Oligocene climate transition, *Paleoceanography*, 26, PA2205, doi:10.1029/2010PA001950, 2011.
- 1189 ~~Rea, D. K. and Lyle, M. W.: Paleogene calcite compensation depth in the eastern subtropical Pacific: Answers and  
 1190 questions. *Paleoceanography*, 20, PA1012, doi:10.1029/2004PA001064, 2005.~~
- 1191 ~~Reichgelt, T., D'Andrea, W. J., & Fox, B. R. Abrupt plant physiological changes in southern New Zealand at the  
 1192 termination of the Mi-1 event reflect shifts in hydroclimate and pCO<sub>2</sub>. *Earth and Planetary Science Letters*, 455,  
 1193 115-124. <https://doi.org/10.1016/j.epsl.2016.09.026>, 2016~~
- 1194 Renaudie, J., Lazarus, D. and Diver, P. NSB (Neptune Sandbox Berlin): An expanded and improved database of marine  
 1195 planktonic microfossil data and deep-sea stratigraphy. *Palaeontologia Electronica*, 23(1):a11  
 1196 <https://doi.org/10.26879/1032>, 2020.
- 1197 ~~Retallack, G. J.: Refining a pedogenic-carbonate CO<sub>2</sub> paleobarometer to quantify a middle Miocene greenhouse spike.  
 1198 *Palaeogeography Palaeoclimatology, Palaeoecology*, 281, 57–65, 2009.~~
- 1199 Rintoul, S.R., Hughes, C.W., Olbers, D. Chapter 4.6 The antarctic circumpolar current system, Editor(s): Gerold Siedler,  
 1200 John Church, John Gould, *International Geophysics*, Academic Press, v.77, 271-XXXVI, 2001.
- 1201 Robert, C., Diester Haass, L. and Chamley, H. (2002). Late Eocene Oligocene oceanographic development at southern  
 1202 high latitudes, from terrigenous and biogenic particles: A comparison of Kerguelen Plateau and Maud Rise, ODP  
 1203 Sites 744 and 689, *Marine Geology*, 191, 37–54, doi:10.1016/S0025-3227(02)00508-X, 2002.
- 1204 Roberts, A.P., Bicknell, S.J., Byatt, J., Bohaty, S.M., Florindo, F., and Harwood, D.M. Magnetostratigraphic calibration  
 1205 of Southern Ocean diatom datums from the Eocene-Oligocene of Kerguelen Plateau (Ocean Drilling Program Sites  
 1206 744 and 748): *Palaeogeography, Palaeoclimatology, Palaeoecology*, v. 198, p. 145–168, doi: 10.1016/S0031-  
 1207 0182(03)00397-3, 2003.
- 1208 ~~Roberts, N.L., Piotrowski, A.M., McManus, J.F., Keigwin, L.D. Synchronous deglacial overturning and water mass  
 1209 source changes. *Science* 84 327, 75e78. <https://doi.org/10.1126/science.1178068>.2010, 2010.~~
- 1210 ~~Roth-Nebelsick, A., Utescher, T., Mosbrugger, V., Diester-Haass, L., and Walther, H.: Changes in atmospheric CO<sub>2</sub>  
 1211 concentrations and climate from the Late Eocene to Early Miocene: palaeobotanical reconstruction based on fossil  
 1212 floras from Saxony, Germany. *Palaeogeography Palaeoclimatology Palaeoecology*, 205, 43–67,  
 1213 <https://doi.org/10.1016/j.palaeo.2003.11.014>, 2004.~~
- 1214 ~~Roth-Nebelsick, A., Grein, M., Utescher, T. and Konrad, W.: Stomatal pore length change in leaves of  
 1215 *Eotrigonobalanus furcinervis* (Fagaceae) from the Late Eocene to the Latest Oligocene and its impact on gas~~

- 1216 [exchange and CO2 reconstruction, \*Rev. Palaeobot. Palynol.\*, 174, 106–112,](#)  
1217 <https://doi.org/10.1016/j.revpalbo.2012.01.001>, 2012.
- 1218 [Roth-Nebelsick, A., Oehm, C., Grein, M., Utescher, T., Kunzmann, L., Friedrich, J.-P., & Konrad, W. Stomatal density](#)  
1219 [and index data of \*Platanus neptuni\* leaf fossils and their evaluation as a CO2 proxy for the Oligocene. \*Review of\*](#)  
1220 [Palaeobotany and Palynology](#), 206, 1–9. <https://doi.org/10.1016/j.revpalbo.2014.03.001>, 2014.
- 1221 Salamy, K.A & Zachos, J.C. Latest Eocene-Early Oligocene climate change and Southern Ocean fertility: inferences  
1222 from sediment accumulation and stable isotope data. *Paleogeography, Paleoclimatology, Paleoecology*, 145, 61–77.  
1223 [https://doi.org/10.1016/S0031-0182\(98\)00093-5](https://doi.org/10.1016/S0031-0182(98)00093-5), 1992.
- 1224 Sarkar, S., Basak, C., Frank, M. Late Eocene onset of the Proto-Antarctic Circumpolar Current. *Science Reports*, 9,  
1225 10125, 2019.
- 1226 Sarmiento, J.L., Gruber, N., Brzezinski, M.A., Dunne, J.P. High-latitude controls of thermocline nutrients and low  
1227 latitude biological productivity. *Nature* 247, 56–60, 2004.
- 1228 Sauermilch, I., Whittaker, J.M., Klocker, A. et al. Gateway-driven weakening of ocean gyres leads to Southern Ocean  
1229 cooling. *Nature Communications* 12, 6465. <https://doi.org/10.1038/s41467-021-26658-1>, 2021.
- 1230 [Shaekleton, N.J. and Opdyke, N.D. Oxygen isotope and paleomagnetic stratigraphy of equatorial Pacific core V28-238:](#)  
1231 [Oxygen isotope temperatures and ice volumes on a 105 year and 106 year scale. \*Quat. Res.\*, 3\(1\), 39-55;](#)  
1232 [doi::10.1016/0033-5894\(73\)90052-5, 1973.](#)
- 1233 [Shaekleton, N. J., and Kennett, P. Paleotemperature history of the Cenozoic and the initiation of Antarctic glaciation:](#)  
1234 [Oxygen and carbon isotope analysis in DSDP Sites 277, 279 and 281, Initial Rep. Deep Sea Drill. Proj., 29, 881–884,](#)  
1235 [1975.](#)
- 1236 [Shaekleton, N.J., Hall, M.A., Boersma, A. Oxygen and carbon isotope data from Leg 74 foraminifers. Init. Rep. Deep](#)  
1237 [Sea Drilling Proj., 74, pp. 599-612, 1984.](#)
- 1238 Scher, H.D. and Martin, E.E. Circulation in the Southern Ocean during the Paleogene inferred from neodymium  
1239 isotopes. *Earth Planet. Sci. Lett.* 228, 391–405. <https://doi.org/10.1016/J.EPSL.2004.10.016>, 2004.
- 1240 Scher, H. D. and Martin, E. E. Timing and climatic consequences of the opening of Drake Passage. *Science*, 312, 428–  
1241 430. DOI: 10.1126/science.1120044, 2006.
- 1242 [Scher H. D., Delaney M. L. Breaking the glass ceiling for high resolution Nd isotope records in early Cenozoic](#)  
1243 [paleoceanography. \*Chem. Geol.\* 269, 329–338. doi: 10.1016/j.chemgeo.2009.10.007, 2010.](#)
- 1244 [Scher, H.D., Bohaty, S.M., Zachos, J.C., Delaney, M.L. Two-stepping into the icehouse: East Antarctic weathering](#)  
1245 [during progressive ice-sheet expansion at the Eocene–Oligocene transition. \*Geology\*, 2011; 39 \(4\): 383–386.](#)  
1246 [doi:https://doi.org/10.1130/G31726.1, 2011](#)
- 1247 Scher, H.D., Bohaty, S.M., Smith, B.W., Munn, G.H. Isotopic interrogation of a suspected late Eocene glaciation.  
1248 *Paleoceanography* 29, 628–644. <https://doi.org/10.1002/2014PA002648>, 2014.
- 1249 Scher, H., Whittaker, J., Williams, S. et al. Onset of Antarctic Circumpolar Current 30 million years ago as Tasmanian  
1250 Gateway aligned with westerlies. *Nature* 523 580–583. <https://doi.org/10.1038/nature14598>, 2015.
- 1251 [Schumacher, S. and Lazarus, D. Regional differences in pelagic productivity in the late Eocene to early Oligocene—a](#)  
1252 [comparison of southern high latitudes and lower latitudes. \*Paleogeography, Paleoclimatology, Paleoecology\*, 214,](#)  
1253 [243-263. https://doi.org/10.1016/j.palaeo.2004.06.018, 2004.](#)
- 1254 [Seton, M., Müller, R., Zahirovic, S., Gaina, C., Torsvik, T., Shephard, G., Talsma, A., Gurnis, M., Turner, M., Maus, S.,](#)  
1255 [and Chandler, M. Global continental and ocean basin reconstructions since 200Ma. \*Earth-Science Reviews\*,](#)  
1256 [113:212-270. https://doi.org/10.1016/j.earscirev.2012.03.002, 2012.](#)
- 1257 [Shackleton, N.J. and Opdyke, N.D. Oxygen isotope and paleomagnetic stratigraphy of equatorial Pacific core V28-238:](#)  
1258 [Oxygen isotope temperatures and ice volumes on a 105 year and 106 year scale. \*Quat. Res.\*, 3\(1\), 39-55.](#)  
1259 [doi::10.1016/0033-5894\(73\)90052-5, 1973.](#)
- 1260 [Shackleton, N. J., and Kennett, P. Paleotemperature history of the Cenozoic and the initiation of Antarctic glaciation:](#)  
1261 [Oxygen and carbon isotope analysis in DSDP Sites 277, 279 and 281, Initial Rep. Deep Sea Drill. Proj., 29, 881–](#)  
1262 [884, 1975.](#)
- 1263 [Shackleton, N.J., Hall, M.A., Boersma, A. Oxygen and carbon isotope data from Leg 74 foraminifers. Init. Rep. Deep](#)  
1264 [Sea Drilling Proj., 74, pp. 599-612, 1984.](#)
- 1265 [Sigman, D. M. & Boyle, E. A. Glacial/interglacial variations in atmospheric carbon dioxide. \*Nature\*, 407, 859–869,](#)  
1266 [2000.](#)
- 1267 [Sigman, D., Hain, M. & Haug, G. The polar ocean and glacial cycles in atmospheric CO2 concentration. \*Nature\*, 466,](#)  
1268 [47–55. https://doi.org/10.1038/nature09149, 2010.](#)
- 1269 [Schumacher, S. and Lazarus, D. Regional differences in pelagic productivity in the late Eocene to early Oligocene—a](#)  
1270 [comparison of southern high latitudes and lower latitudes. \*Paleogeography, Paleoclimatology, Paleoecology\*, 214,](#)  
1271 [243-263. https://doi.org/10.1016/j.palaeo.2004.06.018, 2004.](#)
- 1272 [Seton, M., Müller, R., Zahirovic, S., Gaina, C., Torsvik, T., Shephard, G., Talsma, A., Gurnis, M., Turner, M., Maus, S.,](#)  
1273 [and Chandler, M. Global continental and ocean basin reconstructions since 200Ma. \*Earth-Science Reviews\*, 113:212–](#)  
1274 [270. https://doi.org/10.1016/j.earscirev.2012.03.002, 2012.](#)

- 1275 Sijp, W. P., England, M. H. and Toggweiler, J. R. Effect of Ocean Gateway Changes under Greenhouse Warmth,  
1276 *Journal of Climate*, 22(24), 6639–6652, doi:10.1175/2009JCLI3003.1, 2009.
- 1277 Sijp, W. P., England, M.H., and Huber, M. Effect of the deepening of the Tasman Gateway on the global ocean.  
1278 *Paleoceanography*, 26, doi:10.1029/2011PA002143, 2011.
- 1279 Sijp, W. P., von der Heydt, A. S., and Bijl, P. K.: Model simulations of early westward flow across the Tasman Gateway  
1280 during the early Eocene. *Climate of the Past*, 12, 807–817, <https://doi.org/10.5194/cp-12-807-2016>, 2016.
- 1281 Sluijs, A., Zeebe, R. E., Bijl, P. K., & Bohaty, S. M. A middle Eocene carbon cycle conundrum. *Nature Geoscience*,  
1282 6(6), 429–434. <https://doi.org/10.1038/ngeo1807>, 2013
- 1283 Sokolov, S., Rintoul, S.R. Circumpolar structure and distribution On the relationship between fronts of the Antarctic  
1284 Circumpolar Current fronts: 1. Mean circumpolar paths and surface chlorophyll concentrations in the Southern  
1285 Ocean. *J. Geophys. Res.* 1142, 20097.
- 1286 Srivastava, P., Patel, S., Singh, N., Jamir, T., Kumar, N., Aruche, M., & Patel, R. C. Early Oligocene paleosols of the  
1287 Dagshai Formation, India: A record of the oldest tropical weathering in the Himalayan foreland. *Sedimentary*  
1288 *Geology*, 294, 142-156. <https://doi.org/10.1016/j.sedgeo.2013.05.011>, 2013.
- 1289 Steinthorsdottir, M., Porter, A. S., Holohan, A., Kunzmann, L., Collinson, M., & McElwain, J. C. Fossil plant stomata  
1290 indicate decreasing atmospheric CO<sub>2</sub> prior to the Eocene–Oligocene boundary. *Climate of the Past*, 12(2), 439–  
1291 454. <https://doi.org/10.5194/cp-12-439-2016>, 2016.
- 1292 ~~Sokolov, S., Rintoul, S.R. Circumpolar structure and distribution of the Antarctic Circumpolar Current fronts: 1. Mean~~  
1293 ~~circumpolar paths. *J. Geophys. Res.* 114, 20097.~~
- 1294 Spieß, V. (1990) Cenozoic magnetostratigraphy of Leg 113 drill sites, Maud Rise, Weddell Sea, Antarctica, In: Barker,  
1295 P. F., et al., (eds). Proceedings of the Ocean Drilling Program: College Station, Texas, Scientific Results, v. 113, p. 261–  
1296 318.
- 1297 Stickle, C.E., Brinkhuis, H., Schellenberg, S.A., Sluijs, A., Röhl, U., Fuller, M., Grauert, M., Huber, M., Warnaar, J.,  
1298 Williams, G.L. Timing and nature of the deepening of the Tasmanian Gateway. *Paleoceanography*, 19 (4).  
1299 <https://doi.org/10.1029/2004PA001022>, 2004.
- 1300 Sun, B. N., Wang, Q. J., Konrad, W., Ma, F. J., Dong, J. L., & Wang, Z. X. Reconstruction of atmospheric CO<sub>2</sub> during  
1301 the Oligocene based on leaf fossils from the Ningming Formation in Guangxi, China. *Palaeogeography,*  
1302 *Palaeoclimatology, Palaeoecology*, 467, 5-15. <https://doi.org/10.1016/j.palaeo.2016.09.015>, 2017.
- 1303 Taylor, V. E., Westerhold, T., Bohaty, S.M., Backman, J., Dunkley Jones, T., Edgar, K. M., Egan, K. E., Lyle, M.,  
1304 Pälike, H., Röhl, U., Zachos, J., Wilson, P. A. Transient Shoaling, Over-Deepening and Settling of the Calcite  
1305 Compensation Depth at the Eocene-Oligocene Transition. *Paleoceanography and Palaeoclimatology*, 38(6),  
1306 <https://doi.org/10.1029/2022PA004493>, 2023
- 1307 The Cenozoic CO<sub>2</sub> Proxy Integration Project Consortium, (2023). Toward a Cenozoic History of Atmospheric CO<sub>2</sub>.  
1308 *Science* 382, eadi5177. doi:10.1126/science.adi5177
- 1309 Thole, L.M., Amsler, H.E., Moretti, S., Auderset, A., Gilgannon, J., Lippold, J., Vogel, H., Crosta, X., Mazaud, A.,  
1310 Michel, E., Martínez-García, A., Jaccard, S.L. Glacial- Interglacial dust and export production records from the  
1311 Southern Indian Ocean. *Earth and Planetary Science Letters* 525. <https://doi.org/10.1016/j.epsl.2019.115716>, 2019.
- 1312 Thole, L.M., Amsler, H.E., Moretti, S., Auderset, A., Gilgannon, J., Lippold, J., Vogel, H., Crosta, X., Mazaud, A.,  
1313 Michel, E., Martínez-García, A., Jaccard, S.L. Glacial- interglacial dust and export production records from the  
1314 Southern Indian Ocean. *Earth Planet. Sci. Lett.* 525, 115716. <https://doi.org/10.1016/j.epsl.2019.115716>, 2019.
- 1315 Thomas, E. Late Cretaceous through Neogene deep-sea benthic foraminifera (Maud Rise, Weddell Sea, Antarctica).  
1316 *Proc. Ocean Drill. Program Sci. Results* 113, 571–594, 1990.
- 1317 Toggweiler, J. R. and Samuels, B. Effect of Drake Passage on the global thermohaline circulation. *Deep-Sea Res.* I 42,  
1318 477–500, 1995.
- 1319 Toggweiler, J.R. and Bjornsoon, H. Drake Passage and paleoclimate. *Journal of Quaternary Science*, 15 (4) 319-328.
- 1320 Toumoulin, A., Donnadieu, Y., Ladant, J., Batenburg, S.J., Poblete, F. and Dupont-Nivet, G. (2020). Quantifying the  
1321 Effect of the Drake Passage Opening on the Eocene Ocean. *Paleoceanography and Palaeoclimatology*, 35(8)  
1322 <https://doi.org/10.1029/2020PA003889>, 2000.
- 1323 Van Breedam, J., Huybrechts, P., Crucifix, M. Modelling evidence for late Eocene Antarctic glaciations, *Earth and*  
1324 *Planetary Science Letters*, 586, 117532, ISSN 0012-821X, <https://doi.org/10.1016/j.epsl.2022.117532>, 2022.
- 1325 Vonhof, H.B., Smit, J., Brinkhuis, H., Montanari, A., and Nederbragt, A.J. Global cooling accelerated by early-late  
1326 Eocene impacts: *Geology*, v. 28, p. 687–690, doi: 10.1130/0091-7613(2000)0282.3.CO;2, 2000.
- 1327 Villa, G., Fiorini, C., Persico, D., Roberts, A.P. Florindo, F. Middle Eocene to Late Oligocene Antarctic  
1328 glaciation/deglaciation and Southern Ocean productivity. *Paleoceanography and Palaeoclimatology*, 29, 223-237.  
1329 <https://doi.org/10.1002/2013PA002518>, 2014.
- 1330 Volk, T. and Hoffert, M. I.: Ocean Carbon Pumps: Analysis of Relative Strengths and Efficiencies in Ocean-Driven  
1331 Atmospheric CO<sub>2</sub> Changes, in: The Carbon Cycle and Atmospheric CO<sub>2</sub>: Natural Variations Archean to Present,  
1332 edited by: Sundquist, E. T. and Broecker, W. S., AGU, 99–110, 1985.

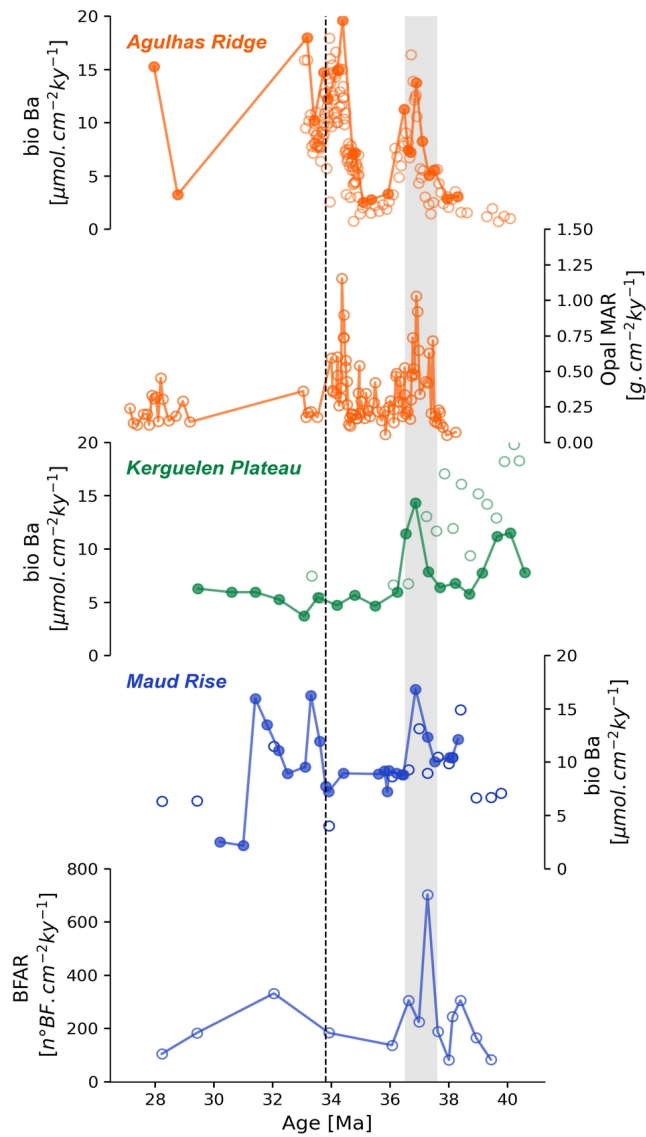
- 1333 | [Vonhof, H.B., Smit, J., Brinkhuis, H., Montanari, A., and Nederbragt, A.J. Global cooling accelerated by early late](#)  
1334 | [Eocene impacts: \*Geology\*, v. 28, p. 687–690, doi: 10.1130/0091-7613\(2000\)0282.3.CO;2, 2000.](#)
- 1335 | Wei, W. Paleogene chronology of Southern Ocean drill holes: An update, in Kennett, J.P., and Warnke, D.A., eds., *The*  
1336 | *Antarctic paleoenvironment: A perspective on global change: Antarctic Research Series*, v. 56, p. 75–96, 1992.
- 1337 | Wei, W., and Wise, S.W. Jr. Eocene-Oligocene calcareous nannofossil magnetobiochronology of the Southern Ocean:  
1338 | *Newsletters on Stratigraphy*, v. 26, p. 119–132, 1992.
- 1339 | Westerhold, T., Marwan, N., Drury, A.J., Liebrand, D., Agnini, C., Anagnostou, E., Barnet, J.S.K., Bohaty, S.M.,  
1340 | Vleeschouwer, Florindo, F., Frederichs, T., Hodell, D.A., Holbourn, A.E., Kroon, D., Laurentino, V., Littler, K.,  
1341 | Lourens, L.J., Lyle, M., Pälike, H., Röhl, U., Tian, J., Wilkens, R.H., Wilson, P.A. and Zachos, J.C. An  
1342 | astronomically dated record of Earth's climate and *itsst* predictability over the last 66 million years. *Science*, 369,  
1343 | 6509, 1383-1387. DOI: 10.1126/science.aba6853, 2020.
- 1344 | Wright, N.M., Scher, H.D., Seton, M., Huck, C.E., Duggan, B.D. No change in Southern Ocean Circulation in the  
1345 | Indian Ocean from the Eocene through Late Oligocene. *Paleoceanography, Paleoclimatology*, 33, 152–167.  
1346 | <https://doi.org/10.1002/2017PA003238>, 2018.
- 1347 | Zachos, C. J., T. M. Quinn, and K. A. Salamy. High-resolution (104 years) deep-sea foraminiferal stable isotope records  
1348 | of the Eocene-Oligocene climate transition, *Paleoceanography*, 11, 251–266, 1996.
- 1349 | Zachos, C. J., B. N. Opdyke, T. M. Quinn, C. E. Jones, and A. N. Halliday. Early Cenozoic glaciation, Antarctic  
1350 | weathering, and seawater  $^{87}\text{Sr}/^{86}\text{Sr}$ : Is there a link? *Chem. Geol.*, 161, 165–180, 1999.
- 1351 | Zachos, J., Pagani, M., Sloan, L., Thomas, E., Billups, K. Trends, rhythms and aberrations in global climate 65 Ma to  
1352 | present. *Science*, 292, 686-693. <https://doi.org/10.1126/science.1059412>, 2001.
- 1353 | Zachos, J., Kump, L. Carbon cycle feedbacks and the initiation of Antarctic glaciation in the earliest Oligocene. *Global*  
1354 | *and Planetary Change*, 47 (1). 51-66 doi:10.1016/j.gloplacha.2005.01.001, 2005.
- 1355 | Zhang, Y. G., Pagani, M., Liu, Z., Bohaty, S. M., and DeConto, R. A 40-million-year history of atmospheric CO<sub>2</sub>.  
1356 | *Philosophical Transactions of the Royal Society A*, v. 371, <https://doi.org/10.1098/rsta.2013.0096>, 2013.



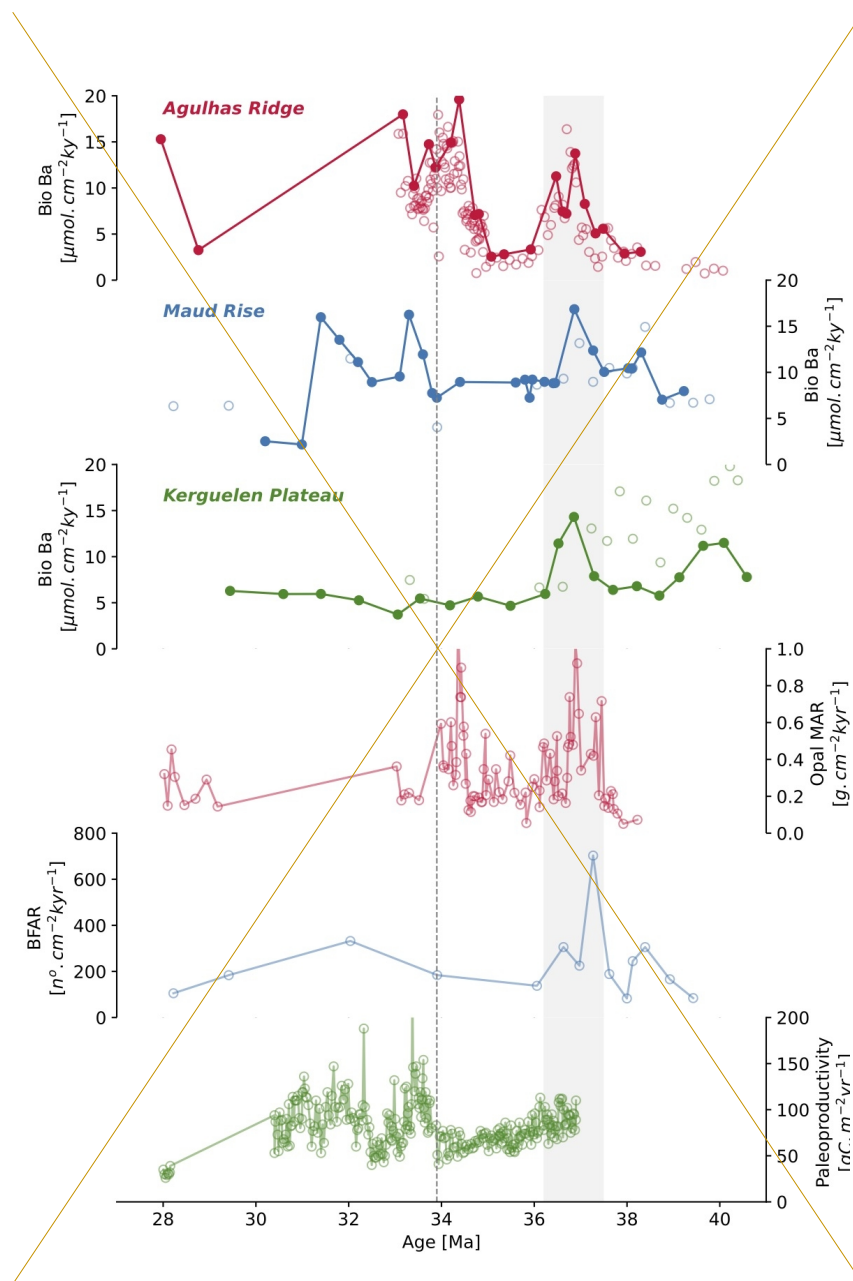




1357 **Figure 1: Schematic Antarctic Circumpolar Current (ACC) and Southern Ocean fronts as determined by Orsi et**  
1358 **al., 1995, named from north to south, STF: Subtropical front, SAF: Subantarctic Front; PF: Polar Front and**  
1359 **SACCF: Southern Antarctic Circumpolar Current Front, and sBdy: Southern Boundary front. Modern location**  
1360 **of ODP sites (1090, Agulhas Ridge; 689, Maud Rise and 748, Kerguelen Plateau) used for reconstructions in this**  
1361 **study. ODP = Ocean Drilling Program.**

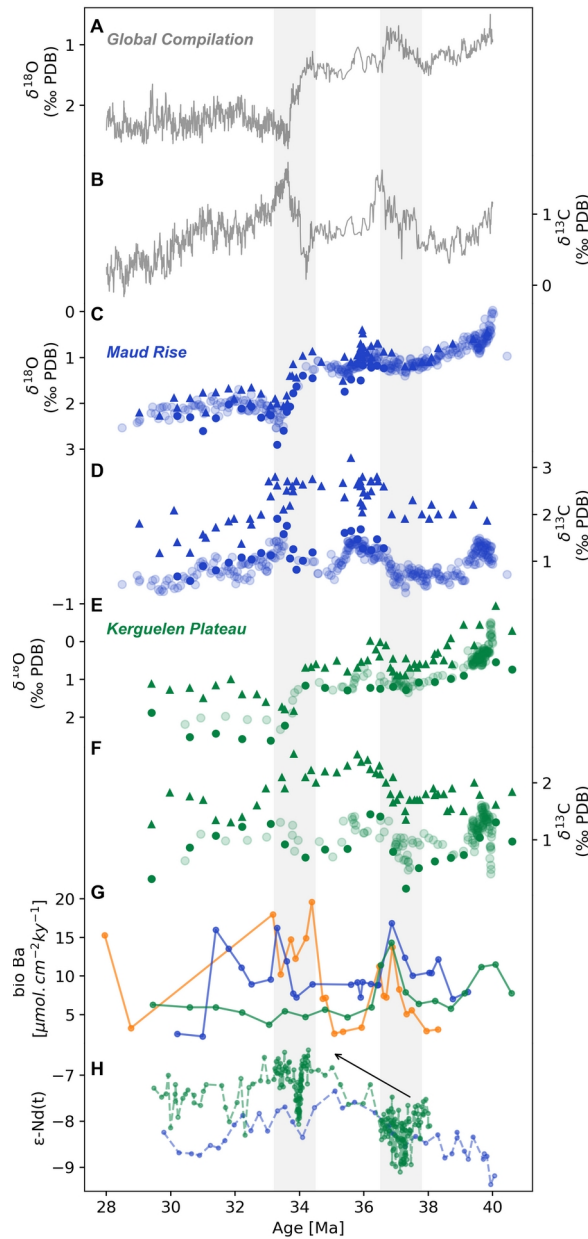


1362 **Figure 2: Paleoproductivity proxies vs Age (Ma) for Agulhas Ridge (ODP Site 1090, in orange), Maud Rise (ODP**  
 1363 **Site 689, in blue) and Kerguelen Plateau (ODP Sites 748, 744, in green). Solid circles are new biogenic barium**  
 1364 **accumulation rate (bio-Ba,  $\mu\text{mol cm}^{-2} \text{kyr}^{-1}$ ) data of this study, open circles from prior literature (Agulhas Ridge**  
 1365 **data from Anderson and Delaney, 2005; Maud Rise data from Diester-Haass and Faul 2019; Kerguelen Plateau**  
 1366 **data from Faul et al., 2010). Site 1090 opal MAR data are from Diekmann et al., 2004. Site 689 BFAR data are**  
 1367 **from Diester-Haass et al., 2019. Vertical bar identifies the E/O boundary (at ca 33.8 Ma). Shaded area**  
 1368 **encompasses the late-Eocene productivity event.**



1369 **Figure 2: Paleoproductivity proxies vs Age (Ma) for Agulhas Ridge (ODP Site 1090, in red), Maud Rise (ODP Site**  
 1370 **689, in blue) and Kerguelen Plateau (ODP Sites 748, 744 and 738, in green). Solid circles are new biogenic**  
 1371 **barium accumulation rate (bio-Ba,  $\mu\text{mol cm}^{-2} \text{kyr}^{-1}$ ) data of this study, open circles from prior literature (Agulhas**  
 1372 **Ridge data from Anderson and Delaney, 2005; Maud Rise data from Diester-Haass and Faul 2019; Kerguelen**  
 1373 **Plateau data from Faul et al., 2010). Site 1090 opal MAR data are from Dickmann et al., 2004. Site 689 BFAR**  
 1374 **data are from Diester-Haass and Zahn 1996. Kerguelen Plateau Site 744 paleoproductivity data from Diester-**

1375 | **Haass (1996). Vertical bar identifies the E/O boundary (at ca 33.8 Ma). Shaded area encompasses the late-Eocene**  
1376 | **productivity event.**

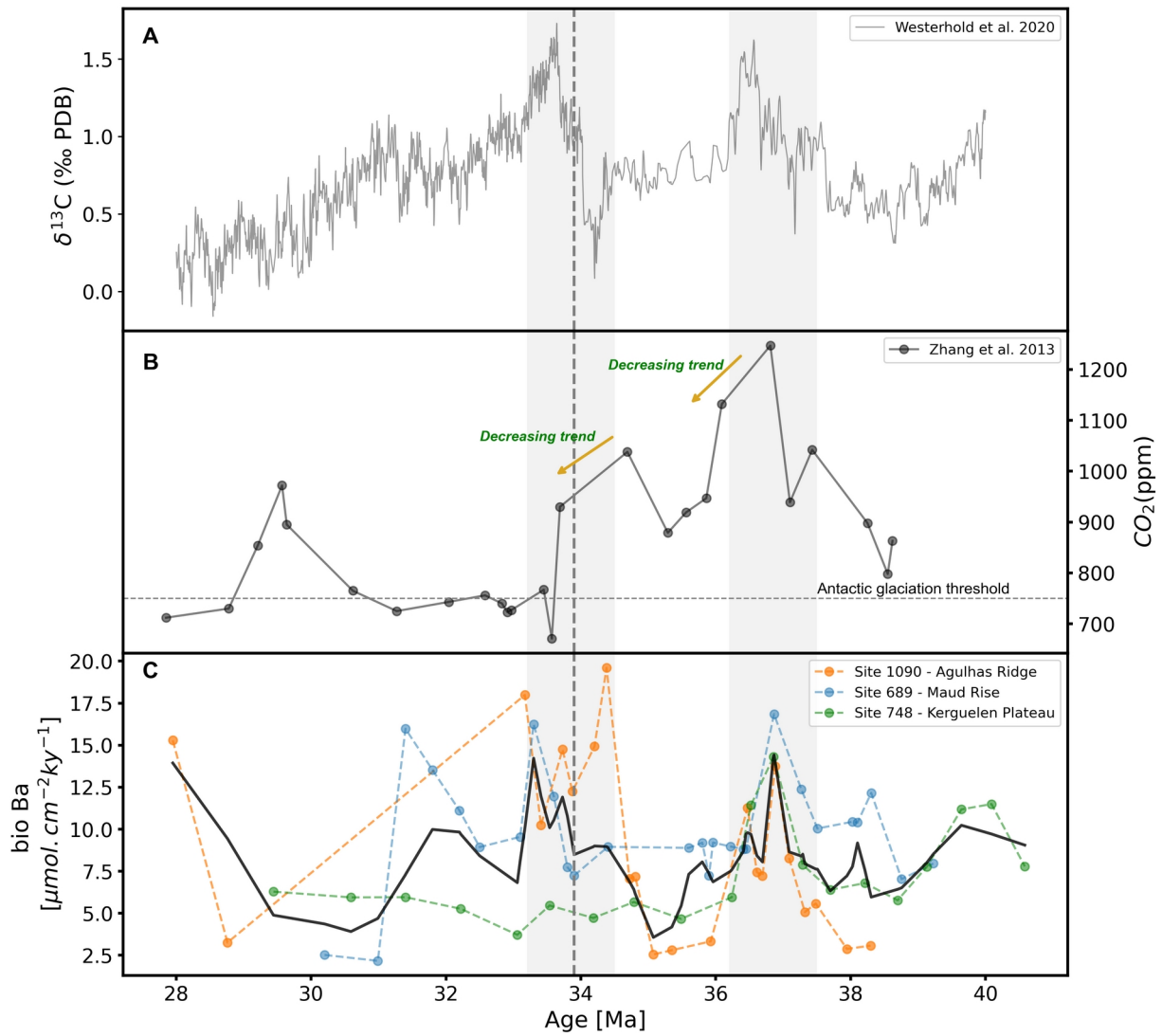


1377 **Figure 3: Multiproxy records from the late Eocene and early Oligocene. Global compilation of oxygen and**  
 1378 **carbon stable isotopes (from Westerhold et al., 2020). New generated oxygen and carbon benthic foraminiferal**  
 1379 **isotopes data (solid circles) and fine fraction (<45μm) (solid triangles), and previously published oxygen and**  
 1380 **carbon stable isotopes (shaded circles, from Mackensen and Ehrmann, 1992; Diester-Haass and Zahn, 1996;**  
 1381 **Bohaty et al., 2003) from Atlantic Southern Ocean (Maud Rise) ODP Site 689 (in blue) and Indian Southern**  
 1382 **Ocean (Kerguelen Plateau) ODP Site 748 (in green). PDB is PeeDee Belemnite carbonate reference. Compilation**  
 1383 **of εNd data obtained from fossil fish teeth for the Atlantic Sector of SO (Maud Rise, in blue, Site 689), and for**  
 1384 **the Indian sector of SO (Kerguelen Plateau, in green, sites 738 and 748) (Scher and Martin, 2004, 2006; Scher et**  
 1385 **al., 2014; Wright et al. 2018). Shaded area identifies E/O boundary at ca 33.8 Ma and productivity event at ca 37**  
 1386 **Ma. Note inverted y-axis scales for oxygen and Nd isotopes.**

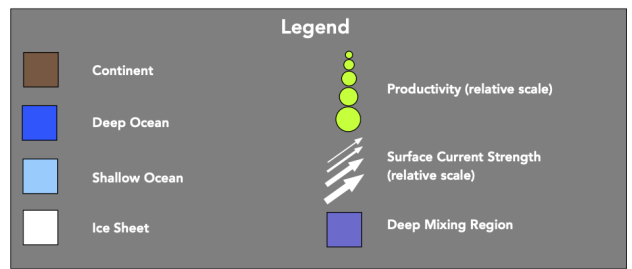
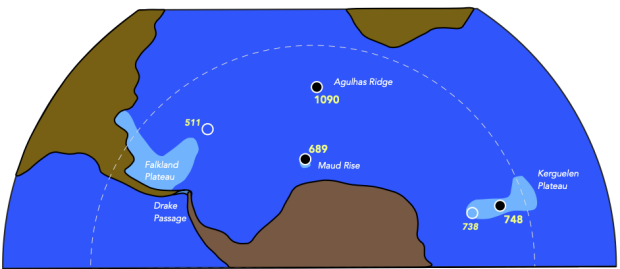
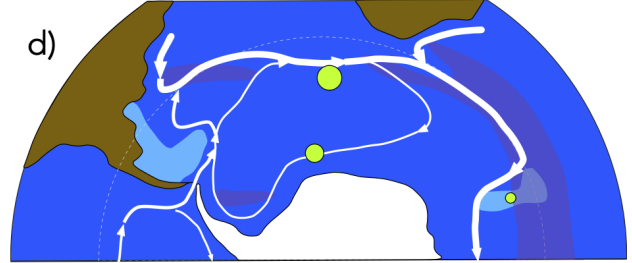
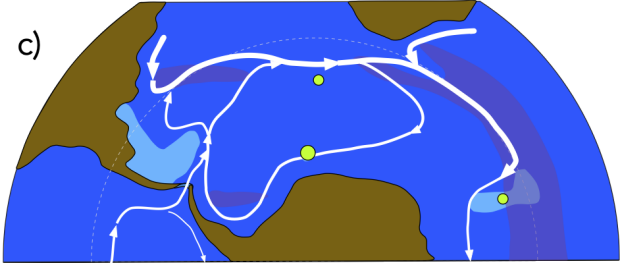
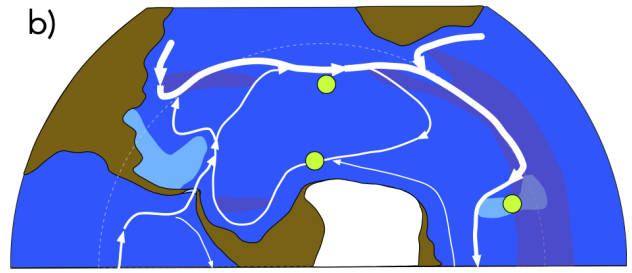
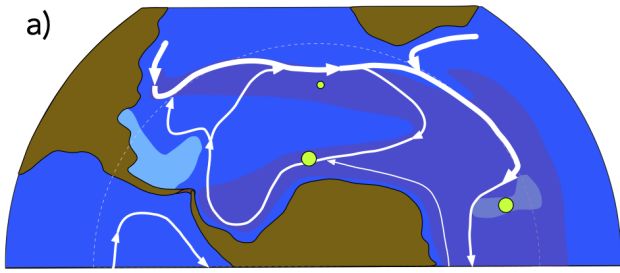


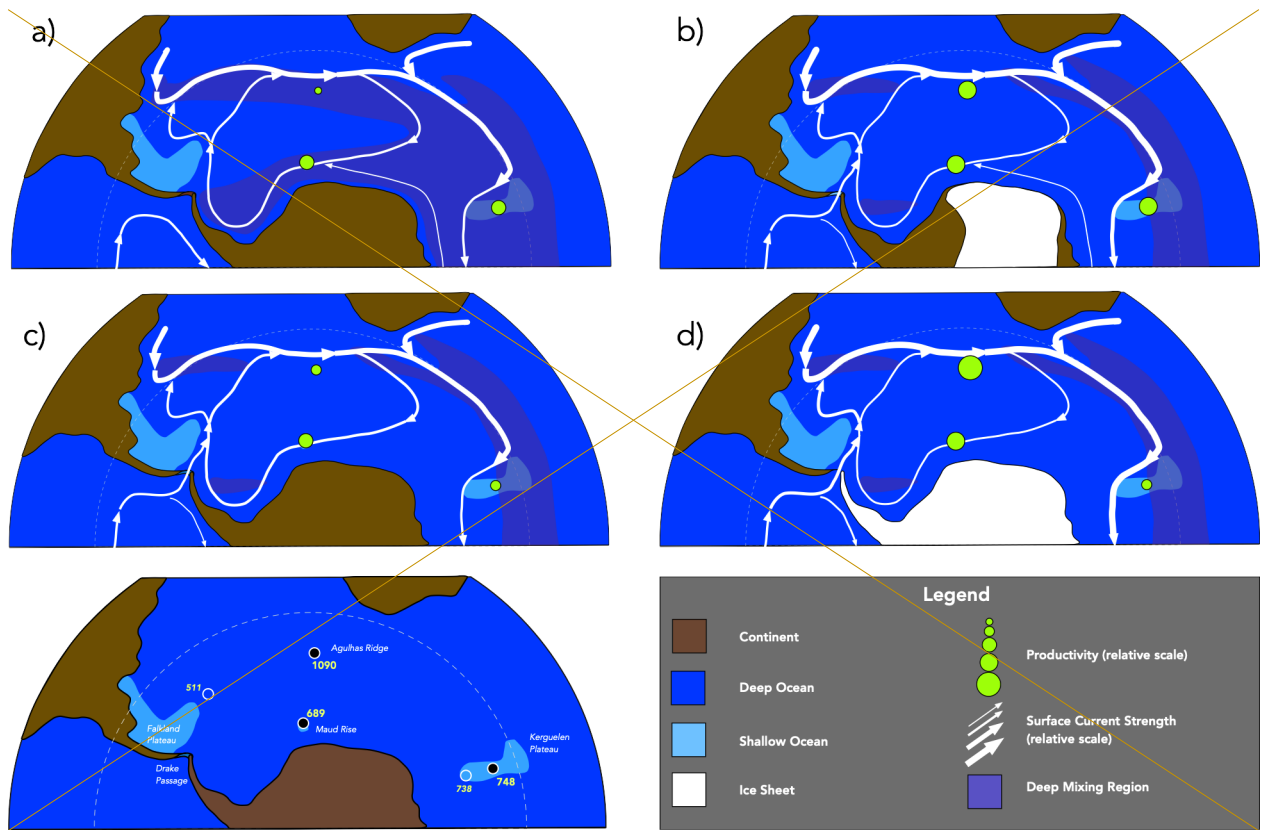
1387 **Figure 3: Multiproxy records from the late Eocene and early Oligocene. Global compilation of oxygen and**  
1388 **carbon stable isotopes (from Westerhold et al., 2020). New generated oxygen and carbon benthic foraminiferal**  
1389 **isotopes data (solid circles) and fine fraction (<45µm) (solid triangles), and previously published oxygen and**  
1390 **carbon stable isotopes (shaded circles, from Mackensen and Ehrmann, 1992; Diester-Haass and Zahn, 1996;**  
1391 **Bohaty et al., 2003) from Atlantic Southern Ocean (Maud Rise) ODP Site 689 (in blue) and Indian Southern**  
1392 **Ocean (Kerguelen Plateau) ODP Site 748 (in green). PDB is Pee Dee Belemnite carbonate reference. Compilation**  
1393 **of  $\epsilon$ Nd data obtained from fossil fish teeth for the Atlantic Sector of SO (Maud Rise – in blue, site 689), and for**  
1394 **the Indian sector of SO (Kerguelen Plateau – in green, sites 738 and 748) (Scher and Martin, 2004, 2006; Scher et**  
1395 **al., 2014; Wright et al. 2018). Shaded area identifies E/O boundary at ca 33.8 Ma and the changes in ocean**  
1396 **circulation. Note inverted y-axis scales for oxygen and Nd isotopes.**

1397 **Figure 4: Comparison between (a) a global compilation of carbon stable isotopes (from Westerhold et al., 2020),**  
1398 **(b) alkenone-based atmospheric  $pCO_2$  record (from Zhang et al., 2013) and (c) biogenic Barium (bio-Ba) export**  
1399 **productivity proxy. Antarctic glaciation thresholds (approx. 750 ppm) (from climate model, DeConto et al. 2008)**  
1400 **is marked by a dashed line. Shaded areas encompass the late Eocene and early Oligocene high productivity**  
1401 **intervals.**



1402 **Figure 4: Comparison between (a) a global compilation of carbon stable isotopes (from Westerhold et al., 2020),**  
 1403 **(b) alkenone-based atmospheric  $p\text{CO}_2$  record (from Zhang et al., 2013) and (c) biogenic Barium (bio-Ba) export**  
 1404 **productivity proxy (this study). Antarctic glaciation thresholds (approx. 750 ppm) (from climate model, DeConto**  
 1405 **et al. 2008) is marked by a dashed line. Shaded areas encompass the late-Eocene and early-Oligocene high**  
 1406 **productivity intervals.**





1407 **Figure 5: Interpretive scenario of paleoceanographic change in the late Eocene to earliest Oligocene Southern**  
 1408 **Ocean. Base map, circulation patterns and extent of deep mixing regions largely after Toumoulin et al. (2020), ice**  
 1409 **sheet extent at 38 Ma after models in Van Breendam (2022). Productivity values based on results of this study,**  
 1410 **shown in relative scale. Note general trend towards higher productivity values, and within this, higher**  
 1411 **productivity, focussed near proto-ACC, during intervals with inferred ice sheets.**